

# A parsimonious neural network approach portfolio optimization problems without using dynamic programming

Pieter M. van Staden\*      Peter A. Forsyth†      Yuying Li‡

December 6, 2023

## Abstract

We discuss a parsimonious neural network approach, which does not rely on dynamic programming techniques, to solve dynamic portfolio optimization problems subject to multiple investment constraints. The approach allows for objectives of a very general form encompassing both time-consistent and time-inconsistent objectives, as well as objectives requiring multi-level optimization. The number of parameters of the neural network remains independent of the number of portfolio rebalancing events. Compared to reinforcement learning, this technique avoids the computation of high-dimensional conditional expectations. The approach remains practical when considering large numbers of underlying assets, long investment time horizons or very frequent rebalancing events. We prove convergence of the numerical solution to the theoretical optimal solution of a large class of problems under fairly general conditions, and present ground truth analyses for a number of popular formulations, including mean-variance, mean-semi-variance, and mean-conditional value-at-risk problems. Numerical experiments show that if the investment objective functional is separable in the sense of dynamic programming, the correct time-consistent optimal investment strategy is recovered, otherwise we obtain the correct pre-commitment (time-inconsistent) investment strategy. This method is agnostic as to the underlying data generating assumptions, and results are illustrated using (i) parametric models for underlying asset returns, (ii) stationary block bootstrap resampling of empirical returns, and (iii) generative adversarial network (GAN)-generated synthetic asset returns.

**Keywords:** Asset allocation, portfolio optimization, neural network, dynamic programming

**JEL classification:** G11, C61

## 1 Introduction

We develop a parsimonious and flexible neural network approach to obtain the numerical solution of a large class of dynamic (i.e. multi-period) portfolio optimization problems, while allowing for multiple investment constraints.

This method presents a significant generalization of our previous work (Li and Forsyth (2019)), and is also related to a large and growing existing literature on the use of neural networks to approximate the optimal control function directly in stochastic optimal control problems, avoiding use of dynamic programming methods (Buehler et al., 2019; Han et al., 2018; Han and Weinan, 2016; Reppen and Soner, 2023; Reppen et al., 2023; Tsang and Wong, 2020). In the taxonomy of Powell (2023), all of these methods are simply variations of the “policy function approximation” approach to stochastic optimal control, and upon cursory inspection are therefore expected to share many common properties.

However, in basic formulation, Buehler et al. (2019); Han and Weinan (2016); Tsang and Wong (2020) rely on a “sub”-neural network to approximate the control at each rebalancing step. Consequently, the number of neural network parameters required increases linearly with the number of portfolio rebalancing events.

Alternatively, a *single* neural network with time as an input feature can be used to approximate the optimal control (Buehler et al., 2019; Li and Forsyth, 2019; Reppen and Soner, 2023; Reppen et al., 2023)). In the taxonomy of Hu and Laurière (2023), these methods can be classified as “global-in-time” machine learning approaches to stochastic control problems. Such an approach implies that the optimal investment strategy at

---

\*National Australia Bank, Melbourne, Victoria, Australia 3000. The research results and opinions expressed in this paper are solely those of the authors, are not investment recommendations, and do not reflect the views or policies of the NAB Group. [pieter.vanstaden@gmail.com](mailto:pieter.vanstaden@gmail.com)

†Cheriton School of Computer Science, University of Waterloo, Waterloo ON, Canada, N2L 3G1, [paforsyt@uwaterloo.ca](mailto:paforsyt@uwaterloo.ca)

‡Cheriton School of Computer Science, University of Waterloo, Waterloo ON, Canada, N2L 3G1, [yuying@uwaterloo.ca](mailto:yuying@uwaterloo.ca)

each rebalancing event would simply involve evaluating the trained neural network by specifying the time and other relevant input features.

Our technique in this paper is *parsimonious*, in the sense that the number of parameters does not scale with the number of rebalancing events. This ensures that our approach remains feasible even for problems with very long time horizons (see e.g. Forsyth et al. (2019)) or with a shorter time horizon but with frequent trading/rebalancing (Forsyth et al., 2011).

Moreover, global-in-time techniques only require the solution of a single optimization problem to determine the parameters of the neural network. This avoids the error amplification problems associated with the backward time-recursion in techniques based on dynamic programming (DP), e.g. Q-learning (Dixon et al., 2020; Gao et al., 2020; Park et al., 2020), or other DP-based techniques (Bachouch et al., 2022; Van Heeswijk and Poutré, 2019).

Given the context of the existing literature, the contributions of this paper are as follows:

- The existing literature focuses on objective functionals that are separable in the sense of dynamic programming, although this may not be required. In this paper, we consider a much larger class of objectives, with generalization along two dimensions:

- (i) We consider objectives of a very general form encompassing both time-consistent and time-inconsistent objectives (see Bjork et al. (2021)). We demonstrate how our method can be used to solve pre-commitment (time-inconsistent) problems to obtain the resulting induced time-consistent strategy (Bjork et al. (2021); Forsyth (2020); Strub et al. (2019a,b)) directly, without first requiring a theoretical derivation of the induced time-consistent problem. Additionally, we demonstrate the application of this method to objectives involving mean-semi-variance (e.g. Sortino ratio), for which no equivalent DP principle is known.

- (ii) We extend the class of objectives considered to include problems involving multi-level optimization such as Mean-CVaR in a dynamic setting (see for example Forsyth (2020); Miller and Yang (2017)). We also allow for a broader class of inner objectives which may not be separable in the sense of dynamic programming.

- We present theoretical results establishing the convergence of the proposed approach for the general class of objectives as discussed above. We prove convergence to the optimal strategy (assuming it exists) in the limit as the number neural network parameters (nodes in each layer) increases, provided that the number of samples in the training data also increases at the appropriate rate.

The broad outlines of our proofs follow along the lines of convergence analyses in the literature (Reppen and Soner, 2023; Tsang and Wong, 2020). However, the details of the convergence proofs differ, in particular due to the nested structure of the objectives and the precise form of the techniques used.

- Numerical examples show that the computed solutions using our technique confirm the theoretical equivalence results regarding the original and embedded formulations of the dynamic Mean-Variance problem. On the other hand, if no equivalent time-consistent formulation exists, then we obtain the correct pre-commitment (time-inconsistent) investment strategy.

The parsimonious neural network approach is also validated by comparing with analytical solutions which assume continuous rebalancing. This demonstrates that the global-in-time approach permits accurate solutions, even for the case of an infinite number of rebalancing times. As a result, our approach can be used without change for both frequent or infrequent rebalancing. We also verify that the approach generates comparable solutions to existing ground truth results for the Mean-CVaR problem.

To emphasize that our approach is independent of any assumptions concerning the underlying data generation method, numerical examples are presented using:

- (i) parametric stochastic models for the underlying asset dynamics,
- (ii) stationary block bootstrap resampling of empirical asset returns,
- (iii) generative adversarial network (GAN)-generated synthetic asset returns.

The remainder of the paper is organized as follows: Section 2 discusses the large class of portfolio optimization problems that can be solved using this methodology, along with issues related to time-consistency and time-inconsistency of the optimal strategies. Section 3 formalizes the problem formulation, while Section 4 provides a

92 summary of the proposed approach, with additional technical and practical details provided in Appendix A and  
 93 Appendix B. Section 5 presents the convergence analysis of the proposed approach. Finally, Section 6 provides  
 94 ground truth analyses, with Section 7 concluding the paper and discussing possible avenues for future research.

## 95 2 Problem overview and selected applications

96 The neural network approach and convergence analysis presented in this paper applies to the solutions of a  
 97 large class of dynamic (i.e. multi-period) portfolio optimization problems that can be expressed in the following  
 98 form,

$$99 \quad \inf_{\xi \in \mathbb{R}} \inf_{\mathcal{P} \in \mathcal{A}} \left\{ E_{\mathcal{P}}^{t_0, w_0} \left[ F(W(T), \xi) + G(W(T), E_{\mathcal{P}}^{t_0, w_0}[W(T)], w_0, \xi) \right] \right\}. \quad (2.1)$$

100 While rigorous definitions and assumptions are discussed in subsequent sections, for introductory purposes we  
 101 simply note that in general,  $F : \mathbb{R}^2 \rightarrow \mathbb{R}$  and  $G : \mathbb{R}^4 \rightarrow \mathbb{R}$  denote some continuous functions and  $\xi \in \mathbb{R}$  some  
 102 auxiliary variable, with  $T > 0$  denoting the investment time horizon,  $W(t), t \in [t_0, T]$ , the controlled wealth  
 103 process, and  $\mathcal{P}$  representing the investment strategy (or control) implemented over  $[t_0, T]$ . Typically,  $\mathcal{P}$  specifies  
 104 the amount or fraction of wealth to invest in each of the underlying assets at each portfolio rebalancing event,  
 105 which in practice occurs at some discrete subset of rebalancing times in  $[t_0, T]$ .  $\mathcal{A}$  denotes the set of admissible  
 106 investment strategies encoding the investment constraints faced by the investor. Finally,  $E_{\mathcal{P}}^{t_0, w_0}[\cdot]$  denotes the  
 107 expectation given control  $\mathcal{P}$  and initial wealth  $W(t_0) = w_0$ .

108 We make the following general observations regarding (2.1):

- 109 • The function  $G$  forming part of the objective is allowed to be a nonlinear function of  $E_{\mathcal{P}}^{t_0, w_0}[W(T)]$ , which  
 110 could result in an optimal control that is not time-consistent (Bjork et al. (2021)). The theoretical and  
 111 practical benefits of solving problems which might be time-inconsistent are discussed in more detail below.
- 112 • For every fixed value of the auxiliary variable  $\xi \in \mathbb{R}$  in the outer optimization problem of (2.1), the inner  
 113 problem  $\inf_{\mathcal{P} \in \mathcal{A}} \{\cdot\}$  takes on the structure of a standard (if possibly time-inconsistent) stochastic optimal  
 114 control problem. As discussed below, this problem structure arises in the case of Mean-Conditional Value-  
 115 at-Risk (CVaR) optimization.
- 116 • Although (2.1) is written for objective functions involving the terminal portfolio wealth  $W(T)$ , the ap-  
 117 proach and convergence analysis could be generalized without difficulty to objective functions that are  
 118 wealth path-dependent, i.e. functions of  $\{W(t) : t \in \mathcal{T}\}$  for some subset  $\mathcal{T} \subseteq [t_0, T]$  - see Forsyth et al.  
 119 (2023); Van Staden et al. (2024) for examples. However, since a sufficiently rich class of problems are of  
 120 the form (2.1), this will remain the main focus of this paper.

121 For purposes of concreteness, we highlight some specific examples of problems of the form (2.1):

- 122 (i) Utility maximization (see for example Vigna (2014)), in which case there is no outer optimization problem  
 123 and  $G \equiv 0$ , while  $w \rightarrow U(w)$  denotes the investor's utility function, so that (2.1) therefore reduces to

$$124 \quad \sup_{\mathcal{P} \in \mathcal{A}} \left\{ E_{\mathcal{P}}^{t_0, w_0} [U(W(T))] \right\}. \quad (2.2)$$

- 125 (ii) Mean-variance (MV) optimization (see e.g. Li and Ng (2000); Zhou and Li (2000)), with  $\rho > 0$  denoting  
 126 the scalarization (or risk aversion) parameter, where the problem

$$127 \quad \sup_{\mathcal{P} \in \mathcal{A}} \left\{ E_{\mathcal{P}}^{t_0, w_0} [W(T)] - \rho \cdot \text{Var}_{\mathcal{P}}^{t_0, w_0} [W(T)] \right\}, \quad (2.3)$$

128 can also be written in the general form (2.1).

- 129 (iii) Mean-CVaR optimization, in which case we do have both an inner and an outer optimization problems  
 130 (see e.g. Forsyth (2020); Miller and Yang (2017), resulting in a problem of the form

$$131 \quad \inf_{\xi \in \mathbb{R}} \inf_{\mathcal{P} \in \mathcal{A}} \left\{ E_{\mathcal{P}}^{t_0, w_0} [F(W(T), \xi)] \right\}, \quad (2.4)$$

132 for a particular choice of the function  $F$  (see (3.15) below).

(iv) To illustrate the flexibility and generality of the proposed approach, we also consider a “mean semi-variance” portfolio optimization problem that is inspired by the popular Sortino ratio (Bodie et al. (2014)) in the case of one-period portfolio analysis, where only the variance of downside outcomes relative to the mean is penalized. In the case of dynamic trading strategies, this suggests an objective function of the form

$$\sup_{\mathcal{P} \in \mathcal{A}} \left\{ E_{\mathcal{P}}^{t_0, w_0} \left[ W(T) - \rho \cdot (\min \{ W(T) - E_{\mathcal{P}}^{t_0, w_0} [W(T)], 0 \})^2 \right] \right\}, \quad (2.5)$$

where, as in the case of (2.3), the parameter  $\rho > 0$  encodes the trade-off between risk and return. Note that (2.5) is not separable in the sense of dynamic programming, and in the absence of embedding results (analogous to those of Li and Ng (2000); Zhou and Li (2000) in the case of MV optimization (2.3)), problem (2.5) cannot be solved using traditional dynamic programming-based methods.

However, we emphasize that (2.2)-(2.5) are only a selection of examples, and the proposed approach and theoretical analysis remains applicable to problems that can be expressed in the general form (2.1).

Portfolio optimization problems of the form (2.1) can give rise to investment strategies that are not time-consistent due to the presence of the (possibly non-linear) function  $G$  (Bjork et al. (2021)). This gives rise to two related problems:

- (i) since (2.1) cannot be solved using a dynamic programming-based approach, some other solution methodology has to be implemented, or some re-interpretation of the problem or the concept of “optimality” might be required (see for example Bjork and Murgoci (2014); Vigna (2022)),
- (ii) if the investment strategies are time-inconsistent, this can raise questions as to whether these strategies are feasible to implement as practical investment strategies.

We make the following general observations:

- It may be desirable to avoid using dynamic programming (DP) even if (2.1) *can* be solved using DP techniques. For example, it is well known that DP has an associated “curse of dimensionality”, in that as the number state variables increases linearly, the computational burden increases exponentially (Fernández-Villaverde et al. (2020); Han and Weinan (2016)). In addition, since DP techniques necessarily incur estimation errors at each time step, significant error amplification can occur which is further exacerbated in high-dimensional settings (Li et al., 2020; Tsang and Wong, 2020; Wang and Foster, 2020).

Instead of relying on DP-based techniques and attempting to address the challenges of dimensionality using machine learning techniques (see for example Bachouch et al. (2022); Dixon et al. (2020); Fernández-Villaverde et al. (2020); Gao et al. (2020); Henry-Labordère (2017); Huré et al. (2021); Lucarelli and Borrotti (2020); Park et al. (2020)), the proposed method fundamentally avoids DP techniques altogether.

This is especially relevant in our setting, since we have shown that in some cases, DP can be *unnecessarily* high-dimensional (see Van Staden et al. (2023)). This occurs since the objective functional (or performance criteria (Oksendal and Sulem (2019))) is typically high-dimensional while the optimal investment strategy remains relatively low-dimensional.

The proposed method therefore forms part of the significant recent interest in developing machine learning techniques to solve multi-period portfolio optimization problems that avoids using DP techniques altogether (see for example Buehler et al. (2019); Ni et al. (2022); Reppen and Soner (2023); Reppen et al. (2023); Tsang and Wong (2020); Van Staden et al. (2023)).

- Time-inconsistent problems naturally arise in financial applications (see Bjork et al. (2021)), and as a result their solution is often an area of active research. Examples include the mean-variance problem, which remained an open problem for decades until the solution using the embedding technique of Li and Ng (2000); Zhou and Li (2000). As a result, being able to obtain a numerical solution to problems of the form (2.1) directly is potentially useful.

From a practical point of view, in many cases, time-inconsistent problems generate an induced time consistent objective function (Forsyth (2020); Strub et al. (2019a,b)). The optimal policy for this induced time consistent objective function is identical to the pre-commitment policy at time zero. The induced time consistent strategy is, of course implementable (Forsyth (2020)), in the sense that the investor has no incentive to deviate from the strategy determined at time zero, at later times.

182 An alternative approach to handling time-inconsistent problems is to search for the equilibrium control  
 183 (Bjork et al. (2021)). A fascinating result obtained in Bjork and Murgoci (2010) is that for every equi-  
 184 librium control, there exists a standard, time consistent problem which has the same control, under a  
 185 different objective function.

186 This essentially means that the question of time-consistency is a often matter of perspective, since there  
 187 may be alternative objective functions which give rise to the same pre-commitment control, yet are time-  
 188 consistent. In fact, other subtle issues arise in comparing pre-commitment and time consistent controls,  
 189 see Vigna (2020, 2022) for further discussion.

190 Furthermore, over very short time horizons such as those encountered in optimal trade execution, time  
 191 consistency or its absence may not be of much concern to the investor or market participant (see for  
 192 example Forsyth et al. (2011); Tse et al. (2013)).

193 In addition, as noted by Bernard and Vanduffel (2014), if the strategy is realized in an investment product  
 194 sold to a retail investor, then the optimal policy from the investor’s point of view is in fact of pre-  
 195 commitment type, since the retail client does not herself trade in the underlying assets during the lifetime  
 196 of the contract.

197 As a result of these observations, we will consider problem (2.1) in its general form. As discussed in the  
 198 Introduction, we present ground truth analyses confirming that the proposed approach is very effective in  
 199 solving portfolio optimization problems of the form (2.1). The results illustrate numerically that if (2.1) is not  
 200 separable in the sense of DP, our approach recovers the correct pre-commitment (time-inconsistent) optimal  
 201 control, otherwise it recovers the correct time-consistent optimal control.

### 202 3 Problem formulation

203 We start by formulating portfolio optimization problems of the form (2.1) more rigorously in a setting of discrete  
 204 portfolio rebalancing and multiple investment constraints. Throughout, we work on filtered probability space  
 205  $(\Omega, \mathcal{F}, \{\mathcal{F}(t)\}_{t \in [t_0, T]}, \mathbb{P})$  satisfying the usual conditions, with  $\mathbb{P}$  denoting the actual (and not the risk-neutral)  
 206 probability measure.

207 Let  $\mathcal{T}$  denote the set of  $N_{rb}$  discrete portfolio rebalancing times in  $[t_0 = 0, T]$ , which we assume to be  
 208 equally-spaced to lighten notation,

$$209 \quad \mathcal{T} = \{t_m = m\Delta t \mid m = 0, \dots, N_{rb} - 1\}, \quad \Delta t = T/N_{rb}, \quad (3.1)$$

210 where we observe that the last rebalancing event occurs at time  $t_{N_{rb}-1} = T - \Delta t$ .

211 At each rebalancing time  $t_m \in \mathcal{T}$ , the investor observes the  $\mathcal{F}(t_m)$ -measurable vector  $\mathbf{X}(t_m) = (X_i(t_m) : i = 1, \dots, \eta_X) \in$   
 212  $\mathbb{R}^{\eta_X}$ , which can be interpreted informally as the information taken into account by the investor in reaching their  
 213 asset allocation decision. As a concrete example, we assume below that  $\mathbf{X}(t_m)$  includes at least the wealth  
 214 available for investment, an assumption which can be rigorously justified using analytical results (see for example  
 215 Van Staden et al. (2023)).

216 Given  $\mathbf{X}(t_m)$ , the investor then rebalances a portfolio of  $N_a$  assets to new positions given by the vector

$$217 \quad \mathbf{p}_m(t_m, \mathbf{X}(t_m)) = (p_{m,i}(t_m, \mathbf{X}(t_m)) : i = 1, \dots, N_a) \in \mathbb{R}^{N_a}, \quad (3.2)$$

218 where  $p_{m,i}(t_m, \mathbf{X}(t_m))$  denotes the fraction of wealth  $W(t_m)$  invested in the  $i$ th asset at rebalancing time  
 219  $t_m$ . The subscript “ $m$ ” in the notation  $\mathbf{p}_m$  emphasizes that in general, each rebalancing time  $t_m \in \mathcal{T}$  could  
 220 be associated with potentially a different function  $\mathbf{p}_m : \mathbb{R}^{\eta_X+1} \rightarrow \mathbb{R}^{N_a}$ , while the subscript is removed below  
 221 when we consider a single function that is simply evaluated at different times, in which case we will write  
 222  $\mathbf{p} : \mathbb{R}^{\eta_X+1} \rightarrow \mathbb{R}^{N_a}$ .

223 For purposes of concreteness, we assume that the investor is subject to the constraints of (i) no short-selling  
 224 and (ii) no leverage being allowed, although the proposed methodology can be adjusted without difficulty to  
 225 treat different constraint formulations<sup>1</sup>. For illustrative purposes, we therefore assume that each allocation (3.2)

---

<sup>1</sup>As discussed in Section 4 and Appendix A, adjustments to the output layer of the neural network may be required.

226 is only allowed to take values in  $(N_a - 1)$ -dimensional probability simplex  $\mathcal{Z}$ ,

$$227 \quad \mathcal{Z} = \left\{ (y_1, \dots, y_{N_a}) \in \mathbb{R}^{N_a} : \sum_{i=1}^{N_a} y_i = 1 \text{ and } y_i \geq 0 \text{ for all } i = 1, \dots, N_a \right\}. \quad (3.3)$$

228 In this setting, an investment strategy or control  $\mathcal{P}$  applicable to  $[t_0, T]$  is therefore of the form,

$$229 \quad \mathcal{P} = \{ \mathbf{p}_m(t_m, \mathbf{X}(t_m)) = (p_{m,i}(t_m, \mathbf{X}(t_m))) : i = 1, \dots, N_a) : t_m \in \mathcal{T} \}, \quad (3.4)$$

230 while the set of admissible controls  $\mathcal{A}$  is defined by

$$231 \quad \mathcal{A} = \{ \mathcal{P} = \{ \mathbf{p}_m(t_m, \mathbf{X}(t_m)) : t_m \in \mathcal{T} \} \mid \mathbf{p}_m(t_m, \mathbf{X}(t_m)) \in \mathcal{Z}, \forall t_m \in \mathcal{T} \}. \quad (3.5)$$

232 The randomness in the system is introduced through the returns of the underlying assets. Specifically, let  
 233  $R_i(t_m)$  denote the  $\mathcal{F}(t_{m+1})$ -measurable return observed on asset  $i$  over the interval  $[t_m, t_{m+1}]$ . We make no  
 234 assumptions regarding the underlying asset dynamics, but at a minimum, we do require  $(\mathbb{P})$  integrability, i.e.  
 235  $\mathbb{E}|R_i(t_m)| < \infty$  for all  $i \in \{1, \dots, N_a\}$  and  $m \in \{0, \dots, N_{rb} - 1\}$ . Informally, we will refer to the set

$$236 \quad \mathbf{Y} = \left\{ (Y_i(t_m) := 1 + R_i(t_m) : i = 1, \dots, N_a)^\top : m \in \{0, \dots, N_{rb} - 1\} \right\} \quad (3.6)$$

237 as the *path* of (joint) asset returns over the investment time horizon  $[t_0, T]$ .

238 To clarify the subsequent notation, for any functional  $\psi(t), t \in [t_0, T]$  we will use the notation  $\psi(t^-)$  and  
 239  $\psi(t^+)$  as shorthand for the one-sided limits  $\psi(t^-) = \lim_{\epsilon \downarrow 0} \psi(t - \epsilon)$  and  $\psi(t^+) = \lim_{\epsilon \downarrow 0} \psi(t + \epsilon)$ , respectively.

240 Given control  $\mathcal{P} \in \mathcal{A}$ , asset returns  $\mathbf{Y}$ , initial wealth  $W(t_0^-) := w_0 > 0$  and a (non-random) cash contribution  
 241 schedule  $\{q(t_m) : t_m \in \mathcal{T}\}$ , the portfolio wealth dynamics for  $m = 0, \dots, N_{rb} - 1$  are given by the general recursion

$$242 \quad W(t_{m+1}^-; \mathcal{P}, \mathbf{Y}) = [W(t_m^-; \mathcal{P}, \mathbf{Y}) + q(t_m)] \cdot \sum_{i=1}^{N_a} p_{m,i}(t_m, \mathbf{X}(t_m)) \cdot Y_i(t_m). \quad (3.7)$$

243 Note that we write  $W(u) = W(u; \mathcal{P}, \mathbf{Y})$  to emphasize the dependence of wealth on the control  $\mathcal{P}$  and the  
 244 (random) path of asset returns in  $\mathbf{Y}$  that relates to the time period  $t \in [t_0, u]$ . In other words, despite using  
 245  $\mathbf{Y}$  in the notation for simplicity,  $W(u; \mathcal{P}, \mathbf{Y})$  is  $\mathcal{F}(u)$ -measurable. Finally, since there are no contributions or  
 246 rebalancing at maturity, we simply have  $W(t_{N_{rb}}^-) = W(T^-) = W(T) = W(T; \mathcal{P}, \mathbf{Y})$ .

### 247 3.1 Investment objectives

248 Given this general investment setting and wealth dynamics (3.7), our goal is to solve dynamic portfolio opti-  
 249 mization problems of the general form

$$250 \quad \inf_{\xi \in \mathbb{R}} \inf_{\mathcal{P} \in \mathcal{A}} J(\mathcal{P}, \xi; t_0, w_0), \quad (3.8)$$

251 where, for some given continuous functions  $F : \mathbb{R}^2 \rightarrow \mathbb{R}$  and  $G : \mathbb{R}^3 \rightarrow \mathbb{R}$ , the objective functional  $J$  is given by

$$252 \quad J(\mathcal{P}, \xi; t_0, w_0) = E_{\mathcal{P}}^{t_0, w_0} \left[ F(W(T; \mathcal{P}, \mathbf{Y}), \xi) + G(W(T; \mathcal{P}, \mathbf{Y}), E_{\mathcal{P}}^{t_0, w_0} [W(T; \mathcal{P}, \mathbf{Y})], w_0, \xi) \right]. \quad (3.9)$$

253 Note that the expectations  $E^{t_0, w_0}[\cdot]$  in (3.9) are taken over  $\mathbf{Y}$ , given initial wealth  $W(t_0^-) = w_0$ , control  $\mathcal{P} \in \mathcal{A}$   
 254 and auxiliary variable  $\xi \in \mathbb{R}$ . In addition to the assumption of continuity of  $F$  and  $G$ , we will make only the  
 255 minimal assumptions regarding the exact properties of  $J$ , including that  $\xi \rightarrow F(\cdot, \xi)$  and  $\xi \rightarrow G(\cdot, \cdot, w_0, \xi)$  are  
 256 convex for all admissible controls  $\mathcal{P} \in \mathcal{A}$ , and the standard assumption (see for example Bjork et al. (2021))  
 257 that an optimal control  $\mathcal{P}^* \in \mathcal{A}$  exists.

258 For illustrative and ground truth analysis purposes, we consider a number of examples of problems of the  
 259 form (3.8)-(3.9).

260 As noted in the Introduction, the simplest examples of problems of the form (3.8) arise in the special  
 261 case where  $G \equiv 0$  and there is no outer optimization problem over  $\xi$ , such as in the case of standard utility  
 262 maximization problems. As concrete examples of this class of objective functions, we will consider the quadratic

263 target minimization (or quadratic utility) described in for example Vigna (2014); Zhou and Li (2000),

$$264 \quad (DSQ(\gamma)) : \quad \inf_{\mathcal{P} \in \mathcal{A}} \left\{ E^{t_0, w_0} \left[ (W(T; \mathcal{P}, \mathbf{Y}) - \gamma)^2 \right] \right\}, \quad \gamma > 0, \quad (3.10)$$

265 as well as the (closely-related) one-sided quadratic loss minimization used in for example Dang and Forsyth  
266 (2016); Li and Forsyth (2019),

$$267 \quad (OSQ(\gamma)) : \quad \inf_{\mathcal{P} \in \mathcal{A}} \left\{ E^{t_0, w_0} \left[ (\min \{W(T; \mathcal{P}, \mathbf{Y}) - \gamma, 0\})^2 - \epsilon \cdot W(T; \mathcal{P}, \mathbf{Y}) \right] \right\}, \quad \gamma > 0. \quad (3.11)$$

268 The term  $\epsilon W(\cdot)$  in equation (3.11) ensures that the problem remains well-posed<sup>2</sup> in the event that  $W(t) \gg \gamma$ .  
269 Observe that problems of the form (3.10) or (3.11) are separable in the sense of dynamic programming, so that  
270 the resulting optimal control is therefore time-consistent.

271 As a classical example of the case where  $G$  is nonlinear and the objective functional (3.9) is not separable  
272 in the sense of dynamic programming, we consider the mean-variance (MV) objective with scalarization or  
273 risk-aversion parameter  $\rho > 0$  (see for example Bjork et al. (2017)),

$$274 \quad (MV(\rho)) : \quad \sup_{\mathcal{P} \in \mathcal{A}} \left\{ E^{t_0, w_0} [W(T; \mathcal{P}, \mathbf{Y})] - \rho \cdot \text{Var}^{t_0, w_0} [W(T; \mathcal{P}, \mathbf{Y})] \right\}, \quad \rho > 0.$$

$$275 \quad = \quad \sup_{\mathcal{P} \in \mathcal{A}} E_{\mathcal{P}}^{t_0, w_0} \left[ W(T; \mathcal{P}, \mathbf{Y}) - \rho \cdot (W(T; \mathcal{P}, \mathbf{Y}) - E_{\mathcal{P}}^{t_0, w_0} [W(T; \mathcal{P}, \mathbf{Y})])^2 \right]. \quad (3.12)$$

276 Note that issues relating to the time-inconsistency of the optimal control of (3.12) are discussed in Remark 3.1  
277 below, along with the relationship between (3.10) and (3.12).

278 As an example of a problem involving both the inner and outer optimization in (3.8), we consider the Mean  
279 - Conditional Value-at-Risk (or Mean-CVaR) problem, subsequently simply abbreviated the MCV problem.  
280 First, as a measure of tail risk, the CVaR at level  $\alpha$ , or  $\alpha$ -CVaR, is the expected value of the worst  $\alpha$  percent  
281 of wealth outcomes, with typical values being  $\alpha \in \{1\%, 5\%\}$ . As in Forsyth (2020), a *larger* value of the CVaR  
282 is preferable to smaller value, since our definition of  $\alpha$ -CVaR is formulated in terms of the terminal *wealth*, not  
283 in terms of the *loss*. Informally, if the distribution of terminal wealth  $W(T)$  is continuous with PDF  $\hat{\psi}$ , then  
284 the  $\alpha$ -CVaR in this case is given by

$$285 \quad \text{CVAR}_{\alpha} = \frac{1}{\alpha} \int_{-\infty}^{w_{\alpha}^*} W(T) \cdot \hat{\psi}(W(T)) \cdot dW(T), \quad (3.13)$$

286 where  $w_{\alpha}^*$  is the corresponding Value-at-Risk (VaR) at level  $\alpha$  defined such that  $\int_{-\infty}^{w_{\alpha}^*} \hat{\psi}(W(T)) dW(T) = \alpha$ .  
287 We follow for example Forsyth (2020) in defining the MCV problem with scalarization parameter  $\rho > 0$  formally  
288 as

$$289 \quad \sup_{\mathcal{P} \in \mathcal{A}} \left\{ \rho \cdot E^{t_0, w_0} [W(T)] + \text{CVAR}_{\alpha} \right\}, \quad \rho > 0. \quad (3.14)$$

290 However, instead of (3.13), we use the definition of CVaR from Rockafellar and Uryasev (2002) that is applicable  
291 to more general terminal wealth distributions, so that the MCV problem definition used subsequently aligns  
292 with the definition given in Forsyth (2020); Miller and Yang (2017)),

$$293 \quad (MCV(\rho)) : \quad \inf_{\xi \in \mathbb{R}} \inf_{\mathcal{P} \in \mathcal{A}} E^{t_0, w_0} \left[ -\rho \cdot W(T; \mathcal{P}, \mathbf{Y}) - \xi + \frac{1}{\alpha} \max(\xi - W(T; \mathcal{P}, \mathbf{Y}), 0) \right], \quad \rho > 0. \quad (3.15)$$

294 Finally, as noted in the Introduction, we apply the ideas underlying the Sortino ratio where the variance of  
295 returns below the mean are penalized, to formulate the following objective function for dynamic trading,

$$296 \quad (MSemiV(\rho)) : \quad \sup_{\mathcal{P} \in \mathcal{A}} \left\{ E_{\mathcal{P}}^{t_0, w_0} \left[ W(T; \mathcal{P}, \mathbf{Y}) - \rho \cdot (\min \{W(T; \mathcal{P}, \mathbf{Y}) - E_{\mathcal{P}}^{t_0, w_0} [W(T; \mathcal{P}, \mathbf{Y})], 0\})^2 \right] \right\}, \quad (3.16)$$

297 which we refer to as the ‘‘Mean- Semi-variance’’ problem, with scalarization (or risk-aversion) parameter  $\rho > 0$ .<sup>3</sup>

298 The following remark discusses issues relating to the possible time-inconsistency of the optimal controls of

<sup>2</sup>Although this is a mathematical necessity (see e.g. (Li and Forsyth, 2019)), in practice, if we use a very small value of  $\epsilon$ , then this has no perceptible effect on the summary statistics. In the numerical results of Section 6, we use  $\epsilon = 10^{-6}$ ; see Appendix B for a discussion.

<sup>3</sup>In continuous time, the unconstrained Mean-Semi-variance problem is ill-posed (Jin et al. (2005)). However, we will impose bounded leverage constraints, which is, of course, a realistic condition. This makes problem (MSemiV( $\rho$ )) well posed.

(3.12) , (3.15) and (3.16).

**Remark 3.1.** (Time-inconsistency and induced time-consistency) Formally, the optimal controls for problems  $MV(\rho)$ ,  $MCV(\rho)$  and  $MSemiV(\rho)$  are not time-consistent, but instead are of the pre-commitment type (see Basak and Chabakauri (2010); Bjork and Murgoci (2014); Forsyth (2020)). However, in many cases, there exists an induced time consistent problem formulation which has the same controls at time zero as the pre-commitment problem (see Forsyth (2020); Strub et al. (2019a,b)).

As a concrete example of induced time-consistency, the embedding result of Li and Ng (2000); Zhou and Li (2000) establishes that the  $DSQ(\gamma)$  objective is the induced time-consistent objective function associated with the  $MV(\rho)$  problem, which is a result that we exploit for ground truth analysis purposes in Section 6.

Similarly, there is an induced time consistent objective function for the Mean-CVAR problem  $MCV(\rho)$  in (3.15) - see Forsyth (2020).

Consequently, when we refer to a strategy as optimal, for either the Mean-CVAR ( $MCV(\rho)$ ) or Mean-Variance ( $MV(\rho)$ ) problems, this will be understood to mean that at any  $t > t_0$ , the investor follows the associated induced time-consistent strategy rather than a pre-commitment strategy.

In the Mean-Semi-variance ( $MSemiV(\rho)$ ) case as per (3.16), there is no obvious induced time consistent objective function. In this case, we seek the pre-commitment policy.

For a detailed discussion of the many subtle issues involved in the case of time-inconsistency, induced time-consistency, and equilibrium controls, see for example Bjork et al. (2021); Bjork and Murgoci (2014); Forsyth (2020); Strub et al. (2019a,b); Vigna (2020, 2022).  $\square$

## 4 Neural network approach

In this section, we provide an overview of the neural network (NN) approach. Additional technical details and practical considerations are discussed in Appendices A and B, while the theoretical justification via convergence analysis will be discussed in Section 5 (and Appendix B).

Recall from (3.2) that  $\mathbf{X}(t_m) \in \mathbb{R}^{\eta_x}$  denotes the information taken into account in determining the investment strategy (3.2) at rebalancing time  $t_m$ . Using the initial experimental results of Li and Forsyth (2019) and the analytical results of Van Staden et al. (2023) applied to this setting, we assume that  $\mathbf{X}(t_m)$  includes at least the wealth available for investment at time  $t_m$ , so that

$$W(t_m^+; \mathcal{P}, \mathbf{Y}) := W(t_m^-; \mathcal{P}, \mathbf{Y}) + q(t_m) \in \mathbf{X}(t_m), \quad \forall t_m \in \mathcal{T}. \quad (4.1)$$

However, we emphasize that  $\mathbf{X}(t_m)$  may include additional variables in different settings. For example, in non-Markovian settings or in the case of certain solution approaches involving auxiliary variables, it is natural to “lift the state space” by including additional quantities in  $\mathbf{X}$  such as relevant historical quantities related to market variables, or other auxiliary variables - see for example Forsyth (2020); Miller and Yang (2017); Tsang and Wong (2020).

Let  $\mathcal{D}_\phi \subseteq \mathbb{R}^{\eta_x+1}$  be the set such that  $(t_m, \mathbf{X}(t_m)) \in \mathcal{D}_\phi$  for all  $t_m \in \mathcal{T}$ . Let  $C(\mathcal{D}_\phi, \mathcal{Z})$  denote the set of all continuous functions from  $\mathcal{D}_\phi$  to  $\mathcal{Z} \subset \mathbb{R}^{N_a}$  (see (3.3)). We will use the notation  $\mathbf{X}^*$  to denote the information taken into account by the optimal control, since in the simplest case implied by (4.1), we simply have  $\mathbf{X}^* = W^*$ , where  $W^*$  denotes the wealth under the optimal strategy. We make the following assumption.

**Assumption 4.1.** (Properties of the optimal control) *Considering the general form of the problem (3.8), we assume that there exists an optimal feedback control  $\mathcal{P}^* \in \mathcal{A}$ . Specifically, we assume that at each rebalancing time  $t_m \in \mathcal{T}$ , the time  $t_m$  itself together with the information vector under optimal behavior  $\mathbf{X}^*(t_m)$ , which includes at least the wealth  $W^*(t_m^+)$  available for investment (see (4.1)), are sufficient to fully determine the optimal asset allocation  $\mathbf{p}_m^*(t_m, \mathbf{X}^*(t_m))$ .*

*Furthermore, we assume that there exists a continuous function  $\mathbf{p}^* \in C(\mathcal{D}_\phi, \mathcal{Z})$  such that  $\mathbf{p}_m^*(t_m, \mathbf{X}^*(t_m)) = \mathbf{p}^*(t_m, \mathbf{X}^*(t_m))$  for all  $t_m \in \mathcal{T}$ , so that the optimal control  $\mathcal{P}^*$  can be expressed as*

$$\mathcal{P}^* = \{\mathbf{p}^*(t_m, \mathbf{X}^*(t_m)) : \forall t_m \in \mathcal{T}\}, \quad \text{where } \mathbf{p}^* \in C(\mathcal{D}_\phi, \mathcal{Z}). \quad (4.2)$$

We make the following observations regarding Assumption 4.1:

- (i) Continuity of  $\mathbf{p}^*$  in space and time: While assuming the optimal control is a continuous map in the state space  $\mathbf{X}$  is fairly standard in the literature, especially in the context of using neural network approximations (see for example Han and Weinan (2016); Huré et al. (2021); Tsang and Wong (2020)), the



assumption of continuity in time in (4.2) is therefore worth emphasizing, since it identifies this approach as a “global in time” approach in the taxonomy of Hu and Laurière (2023), and relates this approach to some specific applications of Buehler et al. (2019); Reppen and Soner (2023); Reppen et al. (2023). This assumption enforces the requirement that in the limit of continuous rebalancing (i.e. when  $\Delta t \rightarrow 0$ ), the control remains a continuous function of time, which is a practical requirement for any reasonable investment policy. In particular, this ensures that the asset allocation retains its smooth behavior as the number of rebalancing events in  $[0, T]$  is increased, which we consider a fundamental requirement ensuring that the resulting investment strategy is reasonable. In addition, in Section 6 we demonstrate how the known theoretical solution to a problem assuming continuous rebalancing ( $\Delta t \rightarrow 0$ ) can be approximated very well using  $\Delta t \gg 0$  in the NN approach, even though the resulting NN approximation is only truly optimal in the case of  $\Delta t \gg 0$ .

- (ii) The control is a *single* function for *all* rebalancing times; note that the function  $\mathbf{p}^*$  is not subscripted by time. If the portfolio is rebalanced only at discrete time intervals, the investment strategy can be found (as suggested in (4.2)) by evaluating this continuous function at discrete time intervals, i.e.  $(t_m, \mathbf{X}(t_m)) \rightarrow \mathbf{p}^*(t_m, \mathbf{X}(t_m)) = (p_i^*(t_m, \mathbf{X}(t_m)) : i = 1, \dots, N_a)$ , for all  $t_m \in \mathcal{T}$ . We discuss below how we solve for this (single) function directly, without resorting to dynamic programming, which avoids not only the challenge with error propagation due to value iteration over multiple timesteps, but also avoids solving for the high-dimensional conditional expectation (also termed the performance criteria by Oksendal and Sulem (2019)) if we are only interested in the relatively low-dimensional optimal control (see for example Van Staden et al. (2023)).

These observations ultimately suggest the NN approach discussed below, while the soundness of Assumption 4.1 is experimentally confirmed in the ground truth results presented in Section 6.

Given Assumption 4.1 and in particular (4.2), we therefore limit our consideration to controls of the form

$$\mathcal{P} = \{\mathbf{p}(t_m, \mathbf{X}(t_m)) : \forall t_m \in \mathcal{T}\}, \quad \text{for some } \mathbf{p} \in C(\mathcal{D}_\phi, \mathcal{Z}). \quad (4.3)$$

To simplify notation, we identify an arbitrary control  $\mathcal{P}$  of the form (4.3) with its associated function  $\mathbf{p} = (p_i : i = 1, \dots, N_a) \in C(\mathcal{D}_\phi, \mathcal{Z})$ , so that the objective functional (3.9) is written as

$$J(\mathbf{p}, \xi; t_0, w_0) = E^{t_0, w_0} \left[ F(W(T; \mathbf{p}, \mathbf{Y}), \xi) + G(W(T), E^{t_0, w_0} [W(T; \mathbf{p}, \mathbf{Y})], w_0, \xi) \right]. \quad (4.4)$$

In (4.4),  $W(\cdot; \mathbf{p}, \mathbf{Y})$  denotes the controlled wealth process using a control of the form (4.3), so that the wealth dynamics (3.7) for  $t_m \in \mathcal{T}$  (recall  $t_{N_r, b}^- = T$ ) now becomes

$$W(t_{m+1}^-; \mathbf{p}, \mathbf{Y}) = [W(t_m^-; \mathbf{p}, \mathbf{Y}) + q(t_m)] \cdot \sum_{i=1}^{N_a} p_i(t_m, \mathbf{X}(t_m)) \cdot Y_i(t_m). \quad (4.5)$$

Therefore, using Assumption 4.1 and (4.4)-(4.5), problem (3.8) is therefore expressed as

$$V(t_0, w_0) = \inf_{\xi \in \mathbb{R}} \inf_{\mathbf{p} \in C(\mathcal{D}_\phi, \mathcal{Z})} J(\mathbf{p}, \xi; t_0, w_0). \quad (4.6)$$

We now provide a brief overview of the proposed methodology to solve problems of the form (4.6). This consists of two steps discussed in the following subsections, namely (i) the NN approximation to the control, and (ii) computational estimate of the optimal control.

## 4.1 Step 1: NN approximation to control

Let  $n \in \mathbb{N}$ . Consider a fully-connected, feedforward NN  $\mathbf{f}_n$  with parameter vector  $\boldsymbol{\theta}_n \in \mathbb{R}^{\nu_n}$  and a fixed number  $\mathcal{L}^h \geq 1$  of hidden layers, where each hidden layer contains  $\bar{h}(n) \in \mathbb{N}$  nodes. The NN has  $(\eta_X + 1)$  input nodes, mapping feature (input) vectors of the form  $\boldsymbol{\phi}(t) = (t, \mathbf{X}(t)) \in \mathcal{D}_\phi$  to  $N_a$  output nodes. For a more detailed introduction to neural networks, see for example Goodfellow et al. (2016).

Additional technical and practical details can be found in Appendices A and B. For this discussion, we simply note that the index  $n \in \mathbb{N}$  is used for the purposes of the analytical results and convergence analysis, where we fix a choice of  $\mathcal{L}^h \geq 1$  while  $\bar{h}(n), n \in \mathbb{N}$  is assumed to be a monotonically increasing sequence such

391 that  $\lim_{n \rightarrow \infty} \bar{h}(n) = \infty$  (see Section 5 and Appendix A). However, for practical implementation, a fixed value  
 392 of  $\bar{h}(n) \in \mathbb{N}$  is chosen (along with  $\mathcal{L}^h \geq 1$ ) to ensure the NN has sufficient depth and complexity to solve the  
 393 problem under consideration (see Appendix B).

394 Any NN considered is constructed such that  $\mathbf{f}_n : \mathcal{D}_\phi \rightarrow \mathcal{Z} \subset \mathbb{R}^{N_a}$ . In other words, the values of the  $N_a$   
 395 outputs are automatically in the set  $\mathcal{Z}$  defined in (3.3) for any  $\phi \in \mathcal{D}_\phi$ ,

$$396 \quad \mathbf{f}_n(\phi(t); \boldsymbol{\theta}_n) = (f_{n,i}(\phi(t); \boldsymbol{\theta}_n) : i = 1, \dots, N_a) \in \mathcal{Z}. \quad (4.7)$$

397 As a result, the outputs of the NN  $\mathbf{f}_n$  in (4.7) can be interpreted as portfolio weights satisfying the required  
 398 investment constraints. While a more detailed discussion of the structure can be found in Assumption A.1 in  
 399 Appendix A, we summarize some key aspects of the NN structure illustrated in Figure 4.1:

- 400 (i) We emphasize that the rebalancing time is an *input* into the NN as per the feature vector  $\phi(t) =$   
 401  $(t, \mathbf{X}(t)) \in \mathcal{D}_\phi$ , so that the NN parameter vector  $\boldsymbol{\theta}_n$  itself does not depend on time.
- 402 (ii) While we assume sigmoid activations for the hidden nodes for concreteness and convenience (see As-  
 403 sumption A.1), any of the commonly-used activation functions can be implemented with only minor  
 404 modifications to the technical results presented in Section 5.
- 405 (iii) Since we are illustrating the approach using the particular form of  $\mathcal{Z}$  in (3.3) because of its wide applica-  
 406 bility (no short-selling and no leverage), a softmax output layer is used to ensure the NN output remains  
 407 in  $\mathcal{Z} \subset \mathbb{R}^{N_a}$  for any  $\phi(t)$  (see (4.7)). However, different admissible control set formulations can be handled  
 408 without difficulty<sup>4</sup>.

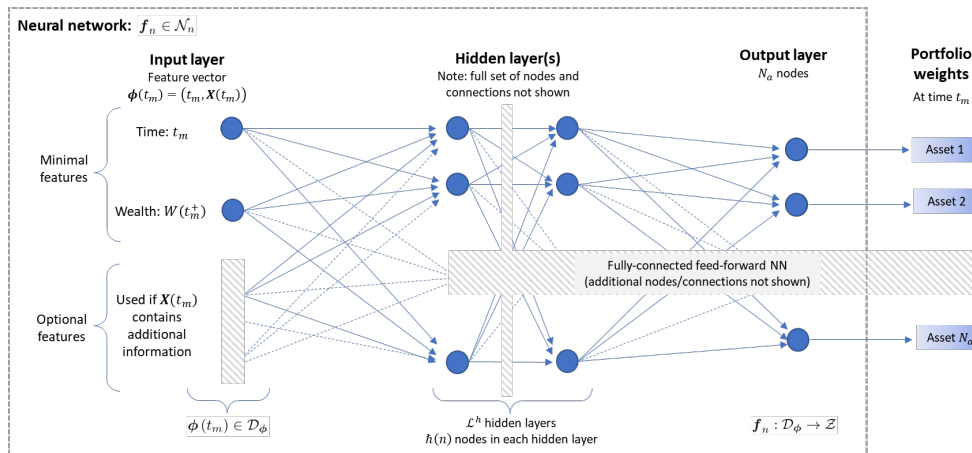


**Figure 4.1:** Illustration of the structure of the NN as per (4.7). Additional construction and implementation details can be found in Appendix A.

409 For some fixed value of the index  $n \in \mathbb{N}$ , let  $\mathcal{N}_n$  denote the set of NNs constructed in the same way as  $\mathbf{f}_n$  for  
 410 the fixed and given values of  $\mathcal{L}^h$  and  $\bar{h}(n)$ . While a formal definition of the set  $\mathcal{N}_n$  is provided in Appendix A,  
 411 here we simply note that each NN  $\mathbf{f}_n(\cdot; \boldsymbol{\theta}_n) \in \mathcal{N}_n$  only differs in terms of the parameter values constituting its  
 412 parameter vector  $\boldsymbol{\theta}_n$  (i.e. for a fixed  $n$ , each  $\mathbf{f}_n \in \mathcal{N}_n$  has the same number of hidden layers  $\mathcal{L}^h$ , hidden nodes  
 413  $\bar{h}(n)$ , activation functions etc.).

414 Observing that  $\mathcal{N}_n \subset C(\mathcal{D}_\phi, \mathcal{Z})$ , our first step is to approximate (4.6) by performing the optimization over  
 415  $\mathbf{f}_n(\cdot; \boldsymbol{\theta}_n) \in \mathcal{N}_n$  instead. In other words, we approximate the control  $\mathbf{p}$  by a neural network  $\mathbf{f}_n \in \mathcal{N}_n$ ,

$$417 \quad \mathbf{p}(\phi(t)) \simeq \mathbf{f}_n(\phi(t); \boldsymbol{\theta}_n), \quad \text{where} \quad \phi(t) = (t, \mathbf{X}(t)), \mathbf{p} \in C(\mathcal{D}_\phi, \mathcal{Z}), \mathbf{f}_n \in \mathcal{N}_n. \quad (4.8)$$

418 We identify the NN  $\mathbf{f}_n(\cdot; \boldsymbol{\theta}_n)$  with its parameter vector  $\boldsymbol{\theta}_n$ , so that the (approximate) objective functional using

<sup>4</sup>For example, position limits and limited leverage can be introduced using minor modifications to the output layer. Perhaps the only substantial challenge is offered by unrealistic investment scenarios, such as insisting that trading should continue in the event of bankruptcy, in which case consideration should be given to the possibility of wealth being identically zero or negative.

419 approximation (4.8) is written as

$$420 \quad J_n(\boldsymbol{\theta}_n, \xi; t_0, w_0) = E^{t_0, w_0} \left[ F(W(T; \boldsymbol{\theta}_n, \mathbf{Y}), \xi) + G(W(T; \boldsymbol{\theta}_n, \mathbf{Y}), E^{t_0, w_0} [W(T; \boldsymbol{\theta}_n, \mathbf{Y})], w_0, \xi) \right]. \quad (4.9)$$

421 Combining (4.7) and (4.8), the wealth dynamics (4.5) is expressed as

$$422 \quad W(t_{m+1}^-; \boldsymbol{\theta}_n, \mathbf{Y}) = [W(t_m^-; \boldsymbol{\theta}_n, \mathbf{Y}) + q(t_m)] \cdot \sum_{i=1}^{N_a} f_{n,i}(\boldsymbol{\phi}(t_m); \boldsymbol{\theta}_n) \cdot Y_i(t_m), \quad m = 0, \dots, N_{rb} - 1. \quad (4.10)$$

423 Using (4.8) and (4.9), for fixed and given values of  $\mathcal{L}^h$  and  $\hbar(n)$ , we therefore approximate problem (4.6) by

$$424 \quad V_n(t_0, w_0) = \inf_{\xi \in \mathbb{R}} \inf_{\mathbf{f}_n(\cdot; \boldsymbol{\theta}_n) \in \mathcal{N}_n} J_n(\boldsymbol{\theta}_n, \xi; t_0, w_0) \quad (4.11)$$

$$425 \quad = \inf_{\xi \in \mathbb{R}} \inf_{\boldsymbol{\theta}_n \in \mathbb{R}^{\nu_n}} J_n(\boldsymbol{\theta}_n, \xi; t_0, w_0)$$

$$426 \quad = \inf_{(\boldsymbol{\theta}_n, \xi) \in \mathbb{R}^{\nu_n+1}} J_n(\boldsymbol{\theta}_n, \xi; t_0, w_0). \quad (4.12)$$

427 We highlight that the optimization in (4.12) is unconstrained since, by construction, each NN  $\mathbf{f}_n(\cdot; \boldsymbol{\theta}_n) \in \mathcal{N}_n$   
428 always generates outputs in  $\mathcal{Z}$ .

429 The notation  $(\boldsymbol{\theta}_n^*, \xi^*)$  and the associated NN  $\mathbf{f}_n^*(\cdot; \boldsymbol{\theta}_n^*) \in \mathcal{N}_n$  are subsequently used to denote the values  
430 achieving the optimum in (4.12) for given values of  $\mathcal{L}^h$  and  $\hbar(n)$ . Note however that we do *not* assume that  
431 the optimal control  $\mathbf{p}^* \in C(\mathcal{D}_\phi, \mathcal{Z})$  satisfying Assumption 4.1 is also a NN in  $\mathcal{N}_n$ , since by the universal  
432 approximation results (see for example Hornik et al. (1989)), we would expect that the error in approximating  
433 (4.6) by (4.12) can be made arbitrarily small for sufficiently large  $\hbar(n)$ . These claims are rigorously confirmed  
434 in Section 5 below, where we consider a sequence of NNs  $\mathbf{f}_n(\cdot; \boldsymbol{\theta}_n) \in \mathcal{N}_n$  obtained by letting  $\hbar(n) \rightarrow \infty$  as  
435  $n \rightarrow \infty$  (for any fixed value of  $\mathcal{L}^h \geq 1$ ).

## 436 4.2 Step 2 : Computational estimate of the optimal control

437 In order to solve the approximation (4.12) to problem (4.6), we require estimates of the expectations in (4.9).  
438 For computational purposes, suppose we take as given a set  $\mathcal{Y}_n \in \mathbb{R}^{n \times N_a \times N_{rb}}$ , consisting of  $n \in \mathbb{N}$  independent  
439 realizations of the paths of joint asset returns  $\mathbf{Y}$ ,

$$440 \quad \mathcal{Y}_n = \left\{ \mathbf{Y}^{(j)} : j = 1, \dots, n \right\}. \quad (4.13)$$

441 We highlight that each entry  $\mathbf{Y}^{(j)} \in \mathcal{Y}_n$  consists of a *path* of joint asset returns (see (3.6)), and we assume that  
442 the paths are independent, we do *not* assume that the asset returns constituting each path are independent. In  
443 particular, both cross-correlations and autocorrelation structures within each path of returns are permitted.

444 Constructing the set  $\mathcal{Y}_n$  in practical applications is further discussed in Appendix B. In the numerical  
445 examples in Section 6, we use examples where  $\mathcal{Y}_n$  is generated using (i) Monte Carlo simulation of parametric  
446 asset dynamics, (ii) stationary block bootstrap resampling of empirical asset returns, (Anarkulova et al. (2022))  
447 and (iii) generative adversarial network (GAN)-generated synthetic asset returns (Yoon et al. (2019)). While  
448 we let  $n \rightarrow \infty$  in (4.13) for convergence analysis purposes, in practical applications (e.g. the results of Section  
449 6) we simply choose  $n$  sufficiently large such that we are reasonably confident that reliable numerical estimates  
450 of the expectations in (4.9) are obtained.

451 Given a NN  $\mathbf{f}_n(\cdot; \boldsymbol{\theta}_n) \in \mathcal{N}_n$  and set  $\mathcal{Y}_n$ , the wealth dynamics (4.10) along path  $\mathbf{Y}^{(j)} \in \mathcal{Y}_n$  is given by

$$452 \quad W^{(j)}(t_{m+1}^-; \boldsymbol{\theta}_n, \mathcal{Y}_n) = [W^{(j)}(t_m^-; \boldsymbol{\theta}_n, \mathcal{Y}_n) + q(t_m)] \cdot \sum_{i=1}^{N_a} f_{n,i}(\boldsymbol{\phi}^{(j)}(t_m); \boldsymbol{\theta}_n) \cdot Y_i^{(j)}(t_m), \quad (4.14)$$

453 for  $m = 0, \dots, N_{rb} - 1$ . We introduce the superscript  $(j)$  to emphasize that the quantities are obtained along the  
454  $j$ th entry of (4.13).

The computational estimate of  $J_n(\boldsymbol{\theta}_n, \xi; t_0, w_0)$  in (4.9) is then given by

$$\begin{aligned} \hat{J}_n(\boldsymbol{\theta}_n, \xi; t_0, w_0, \mathcal{Y}_n) &= \frac{1}{n} \sum_{j=1}^n F\left(W^{(j)}(T; \boldsymbol{\theta}_n, \mathcal{Y}_n), \xi\right) \\ &+ \frac{1}{n} \sum_{j=1}^n G\left(W^{(j)}(T; \boldsymbol{\theta}_n, \mathcal{Y}_n), \frac{1}{n} \sum_{k=1}^n W^{(k)}(T; \boldsymbol{\theta}_n, \mathcal{Y}_n), w_0, \xi\right), \end{aligned} \quad (4.15)$$

so that we approximate problem (4.12) by

$$\hat{V}_n(t_0, w_0; \mathcal{Y}_n) = \inf_{(\boldsymbol{\theta}_n, \xi) \in \mathbb{R}^{\nu_n+1}} \hat{J}_n(\boldsymbol{\theta}_n, \xi; t_0, w_0, \mathcal{Y}_n). \quad (4.16)$$

The numerical solution of (4.16) can then proceed using standard (stochastic) gradient descent techniques (see Appendix B). For subsequent reference, let  $(\hat{\boldsymbol{\theta}}_n^*, \hat{\xi}_n^*)$  denote the optimal point in (4.16) relative to the training data set  $\mathcal{Y}_n$  in (4.16).

In the case of sufficiently large datasets (4.13), in other words as  $n \rightarrow \infty$ , we would expect that the error in approximating (4.12) by (4.16) can be made arbitrarily small. However, as noted above, as  $n \rightarrow \infty$  and the number of hidden nodes  $h(n) \rightarrow \infty$  (for any fixed  $\mathcal{L}^h \geq 1$ ), (4.12) is also expected to approximate (4.6) more accurately. As a result, we obtain the necessary intuition for establishing the convergence of (4.16) to (4.6) under suitable conditions, which is indeed confirmed in the results of Section 5.

Note that since  $\mathcal{Y}_n$  is used in (4.16) to obtain the optimal NN parameter vector  $\hat{\boldsymbol{\theta}}_n^*$ , it is usually referred to as the NN “training” dataset (see for example Goodfellow et al. (2016)). Naturally, we can also construct a “testing” dataset  $\mathcal{Y}_n^{test}$ , that is of a similar structure as (4.13), but typically based on a different implied distribution of  $\mathbf{Y}$  as a result of different data generation assumptions. For example,  $\mathcal{Y}_n^{test}$  can be obtained using a different time period of historical data for its construction, or different process parameters if there are parametric asset dynamics specified. The resulting approximation  $\mathbf{f}_n^*(\cdot; \hat{\boldsymbol{\theta}}_n^*) \in \mathcal{N}_n$  to the optimal control  $\mathbf{p}^* \in C(\mathcal{D}_\phi, \mathcal{Z})$  obtained using the training dataset in (4.16) can then be implemented on the testing dataset for out-of-sample testing or scenario analysis. This is discussed in more detail in Appendix B.

**Remark 4.1.** (Extension to wealth path-dependent objectives) As noted in the Introduction, the NN approach as well as the convergence analysis of Section 5 can be extended to objective functions that depend on the entire wealth path  $\{W(t) : t \in \mathcal{T}\}$  instead of just the terminal wealth  $W(T)$ . This is achieved by simply modifying (4.15) appropriately and ensuring the wealth is assessed at the desired intervals using (4.14).  $\square$

### 4.3 Advantages of the NN approach

The following observations highlight some advantages of the proposed NN approach:

- (i) The approach does not rely on dynamic programming (DP) methods for the solution of problem (4.16), and therefore does not require value iteration or backward time stepping. In particular, we observe that due to the explicit time-dependence of the NN feature vector, the optimization problem (4.16) itself only indirectly depends on the number of rebalancing events, while time recursion is limited to the (computationally inexpensive) wealth dynamics (4.14). As result, problems relating to the error amplification associated with DP methods (Li et al. (2020); Tsang and Wong (2020); Wang and Foster (2020)) are avoided, and only a single optimization problem that is independent of the number of portfolio rebalancing events is solved, in contrast to DP-based methods (see for example Bachouch et al. (2022); Van Heeswijk and Poutré (2019)).

Not relying on DP techniques also makes the approach significantly more flexible, in that it can directly handle objective functions that are not separable in the sense of DP, without requiring theoretical results such as embedding in the case of MV optimization (see for example Li and Ng (2000); Zhou and Li (2000)). As an example of this, we present the solution of the mean - semi-variance problem (3.16) in Section 6.

- (ii) The proposed methodology is parsimonious, in the sense that the NN parameter vector remains independent of number of rebalancing events. Specifically, we observe that the NN parameter vector  $\boldsymbol{\theta}_n \in \mathbb{R}^{\nu_n}$  of the NN does *not* depend on the rebalancing time  $t_m \in \mathcal{T}$  or on the sample path  $j$ . This contrasts our approach with the approaches of for example Han and Weinan (2016); Tsang and Wong (2020),<sup>5</sup> where

<sup>5</sup>Tsang and Wong (2020) use a stacked NN approach, with a different NN at each rebalancing time.

the number of parameters scale with the number of rebalancing events. As a result, the NN approach presented here can lead to potentially significant computational advantages in the cases of (i) long investment time horizons or (ii) short trading time horizons with a frequent number of portfolio rebalancing events.

A natural question might be whether the NNs in the proposed approach are required to be very deep, thus potentially exposing the training of the NN in (4.16) to problem of vanishing or exploding gradients (see for example Goodfellow et al. (2016)). However, the ground truth results presented in Section 6 demonstrate that we obtain very accurate results with relatively shallow NNs (at most two hidden layers). We suspect this might be due to the optimal control being relatively low-dimensional compared to the high-dimensional objective functionals in portfolio optimization problems with discrete rebalancing (see Van Staden et al. (2023) for a rigorous analysis), while in this NN approach the optimal control is obtained directly without requiring the solution of the (high-dimensional) objective functional at rebalancing times.

Note that these advantages also contrast the NN approach with Reinforcement Learning-based algorithms to solve portfolio optimization problems, as the following remark discusses.

**Remark 4.2.** (Contrast of NN approach to Reinforcement Learning). Reinforcement learning (RL) algorithms (for example, Q-learning) relies fundamentally on the DP principle for the numerical solution of the portfolio optimization problem (see for example Gao et al. (2020); Lucarelli and Borrotti (2020); Park et al. (2020)). This requires, at each value iteration step, the approximation of a (high-dimensional) conditional expectation. As a result, RL is associated with standard DP-related concerns related to error amplification and the curse of dimensionality discussed above, and also cannot solve general problems of the form (2.1) without relying on for example an embedding approach to obtain an associated problem that can be solved using DP methods.  $\square$

## 5 Convergence analysis

In this section, we present the theoretical justification of the proposed NN approach as outlined in Section 4. We confirm that the numerical solution of (4.16) can be used to approximate the theoretical solution of (4.6) arbitrarily well (in probability) under suitable conditions. This section only summarizes the key convergence results which are among the main contributions of this paper, while additional technical details and proofs are provided in Appendix A.

We start with Theorem 5.1, which confirms the validity of Step 1 (Subsection 4.1), namely using a NN  $\mathbf{f}_n(\cdot; \boldsymbol{\theta}_n) \in \mathcal{N}_n$  to approximate the control. Note that Theorem 5.1 relies on two assumptions, presented in Appendix A.2: We emphasize that Assumption A.3 is purely made for purposes of convenience, since its requirements can easily be relaxed with only minor modifications to the proofs (as discussed in Remark A.1), but at the cost of significant notational complexity and no additional insights. In contrast, Assumption A.2 is critical to establish the result of Theorem 5.1, and requires that the optimal investment strategy (or control) satisfies Assumption 4.1, places some basic requirements on  $F$  and  $G$ , and assumes that the sequence of NNs  $\{\mathbf{f}_n(\cdot; \boldsymbol{\theta}_n), n \in \mathbb{N}\}$  is constructed such that the number of nodes in each hidden layer  $\bar{h}(n) \rightarrow \infty$  as  $n \rightarrow \infty$  (no assumptions are yet required regarding the exact form of  $n \rightarrow \bar{h}(n)$ ).

**Theorem 5.1.** (Validity of NN approximation) *We assume that Assumption A.2 holds, and for ease of exposition, we also assume that Assumption A.3 holds. Then the NN approximation to the control in (4.8) is valid, in the sense that  $V(t_0, w_0)$  in (4.6) can be approximated arbitrarily well by  $V_n(t_0, w_0)$  in (4.12) for sufficiently large  $n$ , since*

$$\begin{aligned} \lim_{n \rightarrow \infty} |V_n(t_0, w_0) - V(t_0, w_0)| &= \lim_{n \rightarrow \infty} \left| \inf_{(\boldsymbol{\theta}_n, \xi) \in \mathbb{R}^{\nu_n+1}} J_n(\boldsymbol{\theta}_n, \xi; t_0, w_0) - \inf_{\xi \in \mathbb{R}} \inf_{\mathbf{p} \in C(\mathcal{D}_\phi, \mathcal{Z})} J(\mathbf{p}, \xi; t_0, w_0) \right| \\ &= 0. \end{aligned} \tag{5.1}$$

*Proof.* See Appendix A.3.  $\square$

Having justified Step 1 of the approach, Theorem 5.2 now confirms the validity of Step 2 of the NN approach (see Subsection 4.2), namely using the computational estimate  $\mathbf{f}_n^*(\cdot; \hat{\boldsymbol{\theta}}_n^*) \in \mathcal{N}_n$  from (4.16) as an approximation of the true optimal control  $\mathbf{p}^* \in C(\mathcal{D}_\phi, \mathcal{Z})$ . Note that in addition to the assumptions of Theorem 5.1, Theorem 5.2 also requires Assumption A.4, which by necessity includes computational considerations such as the structure

546 of the training dataset  $\mathcal{Y}_n$ , the rate of divergence of the number of hidden nodes  $\hat{h}(n) \rightarrow \infty$  as  $n \rightarrow \infty$ , and  
 547 assumptions regarding the optimization algorithm used in solving problem (4.16).

548 **Theorem 5.2.** (*Validity of computational estimate*) We assume that Assumption A.2, Assumption A.3 and  
 549 Assumption A.4 hold. Then the computational estimate to the optimal control (4.2) obtained using (4.8) and  
 550 (4.16) is valid, in the sense that the value function  $V(t_0, w_0)$  in (4.6) can be approximated arbitrarily well in  
 551 probability by  $\hat{V}_n(t_0, w_0; \mathcal{Y}_n)$  in (4.16) for sufficiently large  $n$ , since

$$552 \quad \left| \hat{V}_n(t_0, w_0; \mathcal{Y}_n) - V(t_0, w_0) \right| = \left| \inf_{(\boldsymbol{\theta}_n, \xi) \in \mathbb{R}^{\eta_n+1}} \hat{J}_n(\boldsymbol{\theta}_n, \xi; t_0, w_0, \mathcal{Y}_n) - \inf_{\xi \in \mathbb{R}} \inf_{\boldsymbol{p} \in C(\mathcal{D}_\phi, \mathcal{Z})} J(\boldsymbol{p}, \xi; t_0, w_0) \right|$$

$$553 \quad \xrightarrow{P} 0, \quad \text{as } n \rightarrow \infty. \quad (5.2)$$

554 *Proof.* See Appendix A.3. □

555 Taken together, Theorem 5.1 and Theorem 5.2 establish the theoretical validity of the NN approach to solve  
 556 problems of the form (2.1).

## 557 6 Numerical results

558 In this section, we present numerical results obtained by implementing the NN approach described in Section  
 559 4. For illustrative purposes, the examples focus on investment objectives as outlined in Subsection 3.1, and we  
 560 use three different data generation techniques for obtaining the training data set  $\mathcal{Y}_n$  of the NN: (i) parametric  
 561 models for underlying asset returns, (ii) stationary block bootstrap resampling of empirical returns, and (ii)  
 562 generative adversarial network (GAN)-generated synthetic asset returns.

### 563 6.1 Closed-form solution: $DSQ(\gamma)$ with continuous rebalancing

564 Under certain conditions, some of the optimization problems in Subsection 3.1 can be solved analytically. In  
 565 this subsection, we demonstrate how a closed-form solution of problem  $DSQ(\gamma)$  in (3.10), assuming *continuous*  
 566 rebalancing (i.e. if we let  $\Delta t \rightarrow 0$  in (3.1)), can be approximated very accurately using a very simple NN  
 567 (1 hidden layer, only 3 hidden nodes) using discrete rebalancing with  $\Delta t \gg 0$  in (3.1). This simultaneously  
 568 illustrates how parsimonious the NN approach is, as well as how useful the imposition of time-continuity is in  
 569 ensuring the smooth behavior of the (approximate) optimal control.

570 In this subsection as well as in Subsection 6.2, we assume parametric dynamics for the underlying assets.  
 571 For concreteness, we consider the scenario of two assets,  $N_a = 2$ , with unit values  $S_i, i = 1, 2$ , evolving according  
 572 to the following dynamics,

$$573 \quad \frac{dS_i(t)}{S_i(t^-)} = \left( \mu_i - \lambda_i \kappa_i^{(1)} \right) \cdot dt + \sigma_i \cdot dZ_i(t) + d \left( \sum_{k=1}^{\pi_i(t)} \left( \vartheta_i^{(k)} - 1 \right) \right), \quad i = 1, 2. \quad (6.1)$$

574 Note that (6.1) takes the form of the standard jump diffusion models in finance - see e.g. Kou (2002);  
 575 Merton (1976) for more information. For each asset  $i$  in (6.1),  $\mu_i$  and  $\sigma_i$  denote the (actual, not risk-neutral)  
 576 drift and volatility, respectively,  $Z_i$  denotes a standard Brownian motion,  $\pi_i(t)$  denotes a Poisson process with  
 577 intensity  $\lambda_i \geq 0$ , and  $\vartheta_i^{(k)}$  are i.i.d. random variables with the same distribution as  $\vartheta_i$ , which represents the jump  
 578 multiplier of the  $i$ th risky asset with  $\kappa_i^{(1)} = \mathbb{E}[\vartheta_i - 1]$  and  $\kappa_i^{(2)} = \mathbb{E}[(\vartheta_i - 1)^2]$ . While the Brownian motions  
 579 can be correlated with  $dZ_1(t) dZ_2(t) = \rho_{1,2} \cdot dt$ , we make the standard assumption that the jump components  
 580 are independent (see for example Forsyth and Vetzal (2022)).

For this subsection only, we treat the first asset ( $i = 1$  in (6.1)) as a “risk-free” asset, and set  $\mu_1 = r > 0$   
 where  $r$  is the risk-free rate, so that we have  $\lambda_1 = 0$ ,  $\sigma_{1j} = 0 \forall j$ , and  $Z_1 \equiv 0$ , while the second asset ( $i = 2$  in  
 (6.1)) is assumed to be a broad equity market index (the “risky asset”). In this scenario, if problem  $DSQ(\gamma)$   
 in (3.10) is solved subject to dynamics (6.1) together with the assumptions of costless continuous trading,  
 infinite leverage, and uninterrupted trading in the event of insolvency, then the  $DSQ(\gamma)$ -optimal control can  
 be obtained analytically as

$$581 \quad \boldsymbol{p}^*(t, W^*(t)) = [1 - p_2^*(t, W^*(t)), p_2^*(t, W^*(t))] \in \mathbb{R}^2, \quad (6.2)$$

**Table 6.1:** Closed-form solution -  $DSQ(\gamma)$  with continuous rebalancing: Percentiles of the simulated ( $n = 2.56 \times 10^6$ ) terminal wealth distributions obtained by implementing the optimal strategies in Figure 6.1. In both cases, a mean terminal wealth of 105 is obtained. Note that the NN approximation was obtained under the assumption of quarterly rebalancing only, no leverage or short-selling, and therefore no trading in insolvency.

Solution approach	Rebalancing	$W(T)$ percentiles				
		5th	20th	50th	80th	95th
Closed-form solution	Continuous, $\Delta t \rightarrow 0$	86.81	98.02	106.35	112.82	118.15
Shallow NN approximation	Discrete, $\Delta t = 0.25$ , total of $N_{rb} = 4$ only	86.62	97.30	105.67	112.54	118.85

where the fraction of wealth in the broad stock market index (asset  $i = 2$ ) is given by (Zweng and Li (2011))

$$p_2^*(t, W^*(t)) = \frac{\mu_2 - r}{\sigma_2^2 + \lambda_2 \kappa_2^{(2)}} \cdot \left[ \frac{\gamma e^{-r(T-t)} - W^*(t)}{W^*(t)} \right], \quad w_0 < \gamma e^{-r(T-t)}. \quad (6.3)$$

581 By design, the NN approach is not constructed to solve problems with unrealistic assumptions such as  
582 continuous trading, infinite leverage and short-selling, or trading in the event of bankruptcy, all of which are  
583 required to derive (6.3). However, if the implicit quadratic wealth target for the DSQ problem (i.e. the value of  
584  $\gamma$ , see Vigna (2014)) is not too aggressive, the analytical solution (6.3) does not require significant leverage or  
585 lead to a large probability of insolvency. In such a scenario, we can use the NN approach to approximate (6.3).

586 We select  $w_0 = 100$ ,  $T = 1$  year and  $\gamma = 138.33$ , and simulate  $n = 2.56 \times 10^6$  paths of the underlying assets  
587 using (6.1) and parameters as in Table C.1 (Appendix C). On this set of paths, the true analytical solution  
588 (6.3) is implemented using 7,200 time steps. In contrast, for the NN approach, we use only 4 rebalancing events  
589 in  $[0, T = 1]$ , and therefore aggregate the simulated returns in quarterly time intervals to construct the training  
590 data set  $\mathcal{Y}_n$ . We consider only a very shallow NN, consisting of a single hidden layer and only 3 hidden nodes.

591 Figure 6.1 compares the resulting optimal investment strategies by illustrating the optimal proportion of  
592 wealth invested in the the broad equity market index (asset  $i = 2$ ) as a function of time and wealth. We  
593 emphasize that the NN strategy in Figure 6.1(b) is not expected to be exactly identical to the analytical  
594 solution in Figure 6.1(a), since it is based on fundamentally different assumptions such as discrete rebalancing  
595 and investment constraints (3.5).

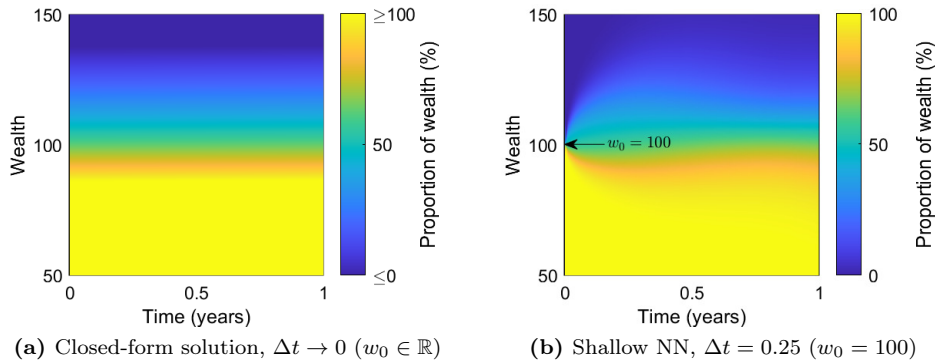


**Figure 6.1:** Closed-form solution -  $DSQ(\gamma)$  with continuous rebalancing: Optimal proportion of wealth invested in the broad equity market index as a function of time and wealth. The NN approximation is obtained for a specific initial wealth of  $w_0 = 100$ , and only four rebalancing events in  $[0, T]$ .

596 However, requiring that the NN feature vector includes time in the proposed NN approach, together with  
597 a NN parameter vector that does not depend on time, we guarantee the smooth behavior in time of the NN  
598 approximation observed in Figure 6.1(b). As a result, Table 6.1 shows that the shallow NN strategy trained  
599 with  $\Delta t \gg 0$  results in a remarkably accurate and parsimonious approximation to the true analytical solution  
600 where  $\Delta t \rightarrow 0$ , since we obtain nearly identical optimal terminal wealth distributions.  
601  
602

## 6.2 Ground truth: Problem $MCV(\rho)$

In the case of the Mean-CVaR problem  $MCV(\rho)$  in (3.15), Forsyth and Vetzal (2022) obtain an MCV-optimal investment strategy subject to the same investment constraints as in Section 3 (namely discrete rebalancing, no short-selling or leverage allowed, and no trading in insolvency) using the partial (integro-)differential equation (PDE) approach of Forsyth (2020).

For ground truth analysis purposes, we therefore consider the same investment scenario as in Forsyth and Vetzal (2022), where two underlying assets are considered, namely 30-day US T-bills and a broad equity market index (the CRSP VWD index) - see Appendix C for definitions. However, in contrast to the preceding section where one asset was taken as the risk-free asset, both assets are now assumed to evolve according to dynamics of the form (6.1), using the double-exponential Kou (2002) formulation for the jump distributions. The NN training data set is therefore constructed by simulating the same underlying dynamics. While further details regarding the context and motivation for the investment scenario can be found in Forsyth and Vetzal (2022), here we simply note that the scenario involves  $T = 5$  years, quarterly rebalancing, a set of admissible strategies satisfying (3.5), and parameters for (6.1) as in Table C.2.

As discussed in Appendix B, the inherently higher complexity of the Mean-CVaR optimal control requires the NN to be deeper than in the case of the problem considered in Subsection 6.1. As a result, we consider approximating NNs with two hidden layers, each with 8 hidden nodes, while relatively large mini-batches of 2,000 paths were used in the stochastic gradient descent algorithm (see Appendix B) to ensure sufficiently accurate sampling of the tail of the returns distribution in selecting the descent direction at each step. Note that despite using a deeper NN, this NN structure is still very parsimonious and relatively shallow compared to the rebalancing time-dependent structures considered in for example Han and Weinan (2016), where a new set of parameters is introduced at each rebalancing event.

Table 6.2 compares the PDE results reported in Forsyth and Vetzal (2022) with the corresponding NN results. Note that the PDE optimal control was determined by solving a Hamilton-Jacobi-Bellman PDE numerically. The statistics for the PDE generated control were computed using  $n = 2.56 \times 10^6$  Monte Carlo simulations of the joint underlying asset dynamics in order to calculate the results of Table 6.2, while the NN was trained on  $n = 2.56 \times 10^6$  paths of the same underlying asset dynamics but which were independently simulated. While some variability of the results are therefore to be expected due to the underlying samples, the results in Table 6.2 demonstrate the robustness of the proposed NN approach.

**Table 6.2:** Ground truth - problem  $MCV(\rho)$ : The PDE results are obtained from Forsyth and Vetzal (2022) for selected points on the Mean-CVaR “efficient frontier”. The “Value function” column reports the value of the objective function (3.14) under the corresponding optimal control, while “% difference” reports the percentage difference in the reported value functions for the NN solution compared to the PDE solution.

$\rho$	5% CVaR		$E^{t_0, w_0} [W(T)]$		Value function		% difference
	PDE	NN	PDE	NN	PDE	NN	
0.10	940.60	940.55	1069.19	1062.97	1047.52	1046.85	-0.06%
0.25	936.23	937.39	1090.89	1081.99	1208.95	1207.88	-0.09%
1.00	697.56	690.11	1437.73	1444.16	2135.29	2134.27	-0.05%
1.50	614.92	611.65	1508.10	1510.07	2877.07	2876.76	-0.01%

## 6.3 Ground truth: Problems $MV(\rho)$ and $DSQ(\gamma)$

In this subsection, we demonstrate that if the investment objective (2.1) is separable in the sense of dynamic programming, the correct time-consistent optimal investment strategy is recovered, otherwise we obtain the correct pre-commitment (time-inconsistent) investment strategy.

To demonstrate this, the theoretical embedding result of Li and Ng (2000); Zhou and Li (2000), which establishes the equivalence of problems  $MV(\rho)$  and  $DSQ(\gamma)$  under fairly general conditions, can be exploited for ground truth analysis purposes as follows. Suppose we solved problems  $MV(\rho)$  and  $DSQ(\gamma)$  on the same underlying training data set. We remind the reader that in the proposed NN approach, problem  $MV(\rho)$  can indeed be solved directly without difficulty, which is not possible in dynamic programming-based approaches. Then, considering the numerical results, there should be values of parameters  $\rho \equiv \tilde{\rho}$  and  $\gamma \equiv \tilde{\gamma}$  such that the optimal strategy of  $MV(\rho \equiv \tilde{\rho})$  corresponds exactly to the optimal strategy of  $DSQ(\gamma \equiv \tilde{\gamma})$ , with a specific



relationship holding between  $\tilde{\rho}$  and  $\tilde{\gamma}$ . The NN approach can therefore enable us to numerically demonstrate the embedding result of Li and Ng (2000); Zhou and Li (2000) in a setting where the underlying asset dynamics are not explicitly specified and where multiple investment constraints are present. We start by recalling the embedding result.

**Proposition 6.1.** (*Embedding result of Li and Ng (2000); Zhou and Li (2000)*) Fix a value  $\tilde{\rho} > 0$ . If  $\mathcal{P}^* \in \mathcal{A}$  is the optimal control of problem  $MV(\rho \equiv \tilde{\rho})$  in (3.12), then  $\mathcal{P}^*$  is also the optimal control for problem  $DSQ(\gamma = \tilde{\gamma})$  in (3.10), provided that

$$\tilde{\gamma} = \frac{1}{2\tilde{\rho}} + E^{t_0, w_0} [W^*(T; \mathcal{P}^*, \mathbf{Y})]. \quad (6.4)$$

*Proof.* See Li and Ng (2000); Zhou and Li (2000). We also highlight the alternative proof provided in Dang and Forsyth (2016), which shows that this result is valid for any admissible control set  $\mathcal{A}$ .  $\square$

Since (6.4) is valid for any admissible control set  $\mathcal{A}$ , we consider a factor investing scenario where portfolios are constructed using popular long-only investable equity factor indices (Momentum, Value, Low Volatility, Size), a broad equity market index (the CRSP VWD index), 30-day T-bills and 10-year Treasury bonds (see Appendix C for definitions). For illustrative purposes in the case of an investor primarily concerned with long-run factor portfolio performance, we use a horizon of  $T = 10$  years,  $w_0 = 120$ , annual contributions of  $q(t_m) = 12$ , and annual rebalancing.

Given historical returns data for the underlying assets, we construct training and testing (out-of-sample) data sets for the NN,  $\mathcal{Y}_n$  and  $\mathcal{Y}_n^{test}$ , respectively, using stationary block bootstrap resampling of empirical historical asset returns (see Appendix C), which is popular with practitioners (Anarkulova et al. (2022); Cavaglia et al. (2022); Cogneau and Zakalmouline (2013); Dichtl et al. (2016); Scott and Cavaglia (2017); Simonian and Martirosyan (2022)) and is designed to handle weakly stationary time series with serial dependence. See Ni et al. (2022) for a discussion concerning the probability of obtaining a repeated path in block bootstrap resampling (which is negligible for any realistic number of samples). Due to availability of historical data we use inflation-adjusted monthly empirical returns from 1963:07 to 2020:12. The training data set ( $n = 10^6$ ) is obtained using an expected block size of 6 months of joint returns from 1963:07 to 2009:12, while the testing data set ( $n = 10^6$ ) uses an expected block size of 3 months and returns from 2010:01 to 2020:12. We consider NNs with two hidden layers, each with only eight hidden nodes.

Choosing two values of  $\tilde{\rho} > 0$  to illustrate different levels of risk aversion (see Table 6.3), we solve problem  $MV(\rho = \tilde{\rho})$  in (3.12) directly using the proposed approach to obtain the optimal investment strategy  $\mathbf{f}(\cdot; \hat{\boldsymbol{\theta}}_{mv}^*)$ . Note that since we consider a fixed NN structure in this setting rather than a sequence of NNs, we drop the subscript “ $n$ ” in the notation  $\mathbf{f}(\cdot; \hat{\boldsymbol{\theta}}_{mv}^*)$ . Using this result together with (6.4), we can approximate the associated value of  $\tilde{\gamma}$  by

$$\tilde{\gamma} \simeq \frac{1}{2\tilde{\rho}} + \frac{1}{n} \sum_{j=1}^n W^{*(j)}(T; \hat{\boldsymbol{\theta}}_{mv}^*, \mathcal{Y}_n), \quad (6.5)$$

and solve problem  $DSQ(\gamma = \tilde{\gamma})$  independently using the proposed approach on the same training data set  $\mathcal{Y}_n$ .

According to Proposition 6.1, the resulting investment strategy  $\mathbf{f}(\cdot; \hat{\boldsymbol{\theta}}_{dsq}^*)$  should be (approximately) identical to the strategy  $\mathbf{f}(\cdot; \hat{\boldsymbol{\theta}}_{mv}^*)$  if the proposed approach works as required. Note that the parameter vectors are expected to be different (i.e.  $\hat{\boldsymbol{\theta}}_{dsq}^* \neq \hat{\boldsymbol{\theta}}_{mv}^*$ ) due to a variety of reasons (multiple local minima, optimization using SGD, etc.), but the resulting wealth distributions and asset allocation should agree, i.e.  $\mathbf{f}(\cdot; \hat{\boldsymbol{\theta}}_{dsq}^*) \simeq \mathbf{f}(\cdot; \hat{\boldsymbol{\theta}}_{mv}^*)$ .

Figure 6.2 demonstrates the investment strategies  $\mathbf{f}(\cdot; \hat{\boldsymbol{\theta}}_{mv}^*)$  and  $\mathbf{f}(\cdot; \hat{\boldsymbol{\theta}}_{dsq}^*)$  obtained by training the NNs on the same training data set using values of  $\tilde{\rho} = 0.017$  and  $\tilde{\gamma} = 429.647$ , respectively. Note that the values  $\tilde{\rho}$  and  $\tilde{\gamma}$  are rounded to three decimal places, and Figure 6.2 corresponds to Results set 1 in Table 6.3. In this example, only four of the underlying candidate assets have non-zero investments, which is to be expected due to the high correlation between long-only equity factor indices.

Table 6.3 confirms that the associated optimal terminal wealth distributions of  $MV(\rho = \tilde{\rho})$  and  $DSQ(\gamma = \tilde{\gamma})$  indeed correspond, both in-sample (training data set) and out-of-sample (testing data set).

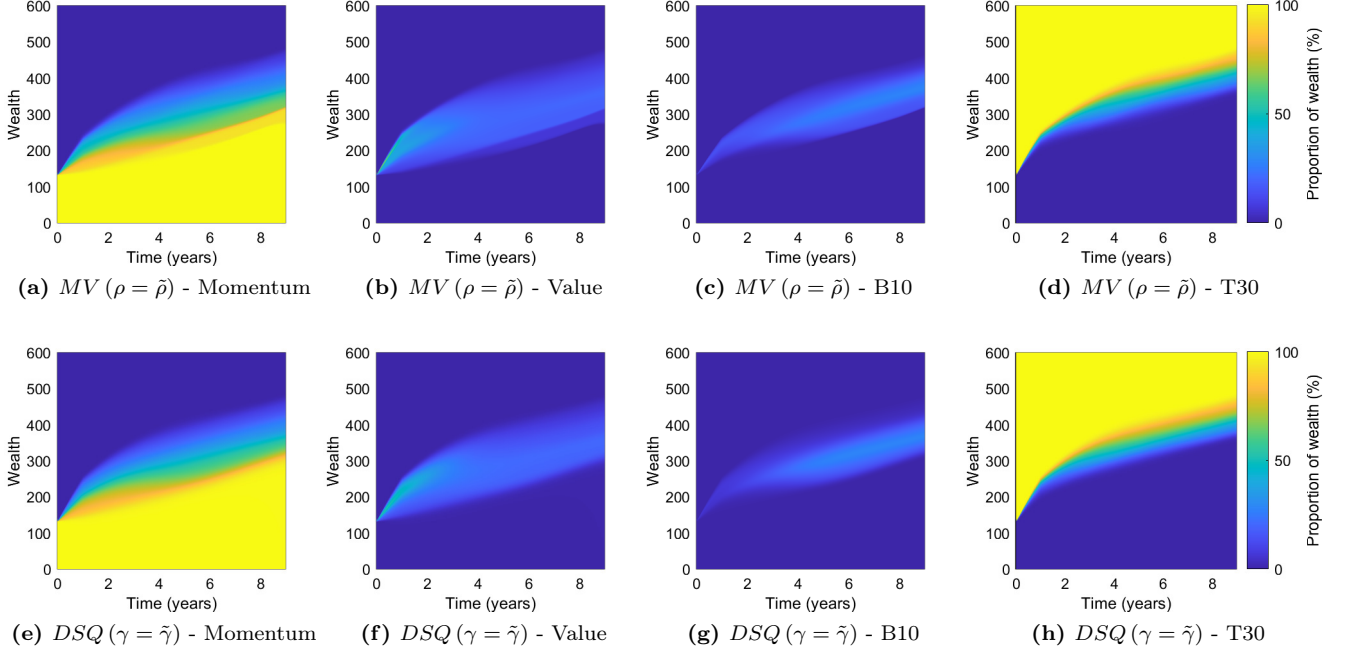


**Figure 6.2:** Ground truth - problems  $MV(\rho = \tilde{\rho})$  and  $DSQ(\gamma = \tilde{\gamma})$ : investment strategies  $\mathbf{f}(\cdot; \hat{\theta}_{mv}^*)$  and  $\mathbf{f}(\cdot; \hat{\theta}_{dsq}^*)$  obtained by training the NNs using values of  $\tilde{\rho} = 0.017$  and  $\tilde{\gamma} = 429.647$  (rounded to three decimal places), respectively. Each figure shows the proportion of wealth invested in the asset as a function of the minimal NN features, namely time and available wealth. Zero investment under the optimal strategies in the broad market index and the Size factor.

**Table 6.3:** Ground truth - problems  $MV(\rho = \tilde{\rho})$  and  $DSQ(\gamma = \tilde{\gamma})$ : Terminal wealth results obtained using  $n = 10^6$  joint paths for the underlying assets. Note that the values of  $\tilde{\rho}$  and  $\tilde{\gamma}$  are rounded to three decimal places, .

$W(T)$ distribution	Results set 1: $\tilde{\rho} = 0.017, \tilde{\gamma} = 429.647$				Results set 2: $\tilde{\rho} = 0.0097, \tilde{\gamma} = 493.196$			
	Training data		Testing data		Training data		Testing data	
	MV	DSQ	MV	DSQ	MV	DSQ	MV	DSQ
Mean	400.2	400.3	391.2	391.6	441.5	441.8	441.8	441.5
Stdev	55.4	55.4	26.2	25.7	79.6	79.7	39.4	39.5
5th percentile	276.5	276.4	346.6	347.5	255.2	254.6	367.8	367.1
25th percentile	391.8	392.3	382.4	382.8	422.4	423.6	430.9	430.7
50th percentile	416.1	416.3	396.5	396.8	469.8	470.1	451.3	451.2
75th percentile	429.9	429.8	406.4	406.7	487.7	489.6	465.0	464.8
95th percentile	452.1	452.1	418.9	419.0	516.1	516.5	480.9	480.2

691 The proposed NN approach therefore clearly works as expected, in that we demonstrated that the result  
692 of Proposition 6.1 in a completely model-independent way in a portfolio optimization setting where no known  
693 analytical solutions exist. In particular, we emphasize that no assumptions were made regarding parametric  
694 underlying asset dynamics, the results are entirely data-driven. As a result, we can interpret the preceding  
695 results as showing that the approach correctly recovers the time-inconsistent (or pre-commitment) strategy  
696 without difficulty if the objective is not separable in the sense of dynamic programming, such as in the case of  
697 the  $MV(\rho)$  problem, whereas if the objective is separable in the sense of dynamic programming, such as in the  
698 case of the  $DSQ(\gamma)$  problem, the approach correctly recovers the associated time-consistent strategy.

## 699 6.4 Mean - Semi-variance strategies

700 Having demonstrated the reliability of the results obtained using the proposed NN approach with the preceding  
701 ground truth analyses, we now consider the solution of the Mean - Semi-variance problem (3.16). To provide the  
702 necessary context to interpret the  $MSemiV(\rho)$ -optimal results, we compare the results of the optimal solutions  
703 of the  $MCV(\rho = \rho_{mcv})$ ,  $MSemiV(\rho = \rho_{msv})$ , and  $OSQ(\gamma = \gamma_{osq})$  problems, where the values of  $\rho_{mcv}$ ,  $\rho_{msv}$   
704 and  $\gamma_{osq}$  are selected to obtain the same expected value of terminal wealth on the NN training data set. This  
705 is done since the MCV- and OSQ-optimal strategies have been analyzed in great detail (Dang and Forsyth

(2016); Forsyth (2020)), and are therefore well understood. Note that since all three strategies are related to the maximization of the mean terminal wealth and while simultaneously minimizing some risk measure (which is implicitly done in the case of the OSQ problem, see Dang and Forsyth (2016)), it is natural to compare the strategies on the basis of equal expectation of terminal wealth.

To highlight the main qualitative features of the  $MSemiV(\rho)$ -optimal results, we consider a simple investment scenario of two assets, namely 30-day T-bills and a broad equity market index (the VWD index) - see Appendix C for definitions. We choose  $T = 5$  years,  $w_0 = 1000$ , and zero contributions to demonstrate a lump sum investment scenario with quarterly rebalancing.

To illustrate the flexibility of the NN approach to underlying data generating assumptions, the NN training data sets are constructed using generative adversarial network (GAN)-generated synthetic asset returns obtained by implementing the TimeGAN algorithm proposed by Yoon et al. (2019). In more detail, using empirical monthly asset returns from 1926:01 to 2019:12 for the underlying assets (data sources are specified in Appendix C), the TimeGAN is trained with default parameters as in Yoon et al. (2019) using block sizes of 6 months to capture both correlation and serial correlation aspects of the (joint) time series.<sup>6</sup> Once trained, the TimeGAN is then used to generate a set of  $n = 10^6$  paths of synthetic asset returns, which is used as the training data set to train the NNs corresponding to the MCV, MSemiV and OSQ-optimal investment strategies.

Figure 6.3 illustrates the resulting optimal investment strategies, and we observe that the MSemiV-optimal strategy is fundamentally different from the MCV and OSQ-optimal strategies, while featuring elements of both. Specifically, Figure 6.4, which illustrates the resulting optimal terminal wealth distributions (with the same expectation), demonstrates that the MSemiV strategy, like the MCV strategy, can offer better downside protection than the OSQ strategy, while the MSemiV strategy retains some of the qualitative elements of the OSQ distribution such as the left skew.

Having illustrated that the MSemiV problem can be solved in a dynamic trading setting using the proposed NN approach to obtain investment strategies that offer potentially valuable characteristics, we leave a more in-depth investigation of the properties and applications of MSemiV-optimal strategies for future work.

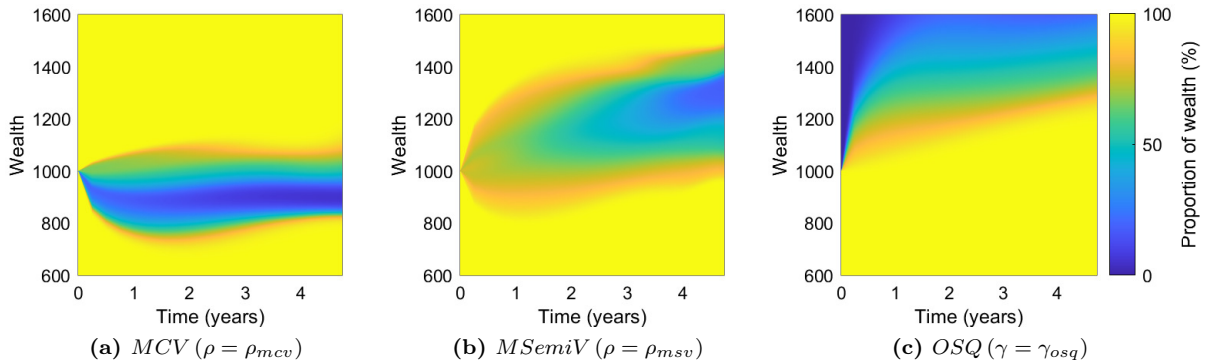


**Figure 6.3:** Optimal investment strategies for the  $MCV(\rho = \rho_{mcv})$ ,  $MSemiV(\rho = \rho_{msv})$ , and  $OSQ(\gamma = \gamma_{osq})$  strategies, obtaining identical expectation of terminal wealth on the training data set. Each figure shows the proportion of wealth invested in the broad equity market index as a function of the minimal NN features, namely time and available wealth.

731

732

## 7 Conclusion

733

In this paper, we presented a flexible NN approach, which does not rely on dynamic programming techniques, to solve a large class of dynamic portfolio optimization problems. We considered objectives of a very general form,

734

735

<sup>6</sup>It appears that the actual code in Yoon et al. (2019) implements the following steps: (i) takes as input actual price data, (ii) forms rolling blocks of price data and (iii) forms a single synthetic price path (which is the same length as the original path) by randomly sampling (without replacement) from the set of rolling blocks. Step (iii) corresponds to the non-overlapping block bootstrap using a fixed block size. This should be contrasted with stationary block bootstrap resampling of Politis and Romano (1994). Step (i) does not make sense as input to a bootstrap technique, since the data set is about 10 years long, with an initial price of \$50 and a final price of \$1200. We therefore changed Step (i), so that all data was converted to returns prior to being used as input.

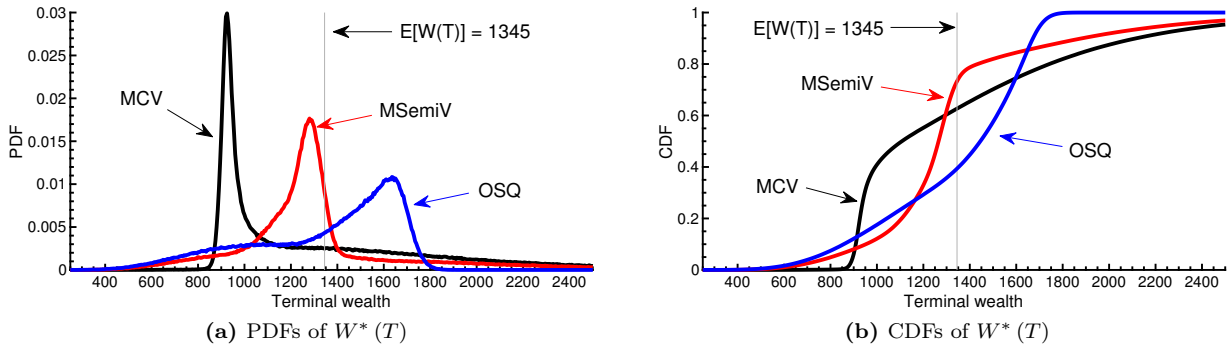


**Figure 6.4:** PDFs and CDFs of optimal terminal wealth obtained under the *MCV* ( $\rho = \rho_{mcv}$ ), *MSemiV* ( $\rho = \rho_{msv}$ ), and *OSQ* ( $\gamma = \gamma_{osq}$ ) strategies, where the values of  $\rho_{mcv}$ ,  $\rho_{msv}$  and  $\gamma_{osq}$  are selected to obtain the same expected value of optimal terminal wealth on the NN training data set.

736 encompassing both time-consistent and time-inconsistent objectives, as well as objectives requiring multi-level  
 737 optimization. In the proposed approach, a single optimization problem is solved, issues of instability and error  
 738 propagation involved in estimating high-dimensional conditional expectations are avoided, and the resulting  
 739 NN is parsimonious in the sense that the number of parameters does not scale with the number of rebalancing  
 740 events.

741 We also presented theoretical convergence analysis results which show that the numerical solution obtained  
 742 using the proposed approach can recover the optimal investment strategy, provided it exists, regardless of  
 743 whether the resulting optimal investment strategy is time-consistent or (formally) time-inconsistent.

744 Numerical results confirmed the advantages of the NN approach, and showed that accurate results can be  
 745 obtained in ground truth analyses in a variety of settings. The numerical results also highlighted that the  
 746 approach remains agnostic as to the underlying data generating assumptions, so that for example empirical  
 747 asset returns or synthetic asset returns can be used without difficulty.

748 We conclude by noting that the NN approach is not necessarily limited to portfolio optimization problems  
 749 such a those encountered during the accumulation phase of pension funds, and could be extended to address  
 750 the significantly more challenging problems encountered during the decumulation phase of defined contribution  
 751 pension funds (see for example Forsyth (2022)). We leave this extension for future work.

## 752 8 Declarations

753 The authors have no competing interests to declare that are relevant to the content of this article.

## 754 9 Acknowledgements

755 P.A. Forsyth’s work was supported by the Natural Sciences and Engineering Research Council of Canada  
 756 (NSERC) grant RGPIN-2017-03760. Li’s work was supported by the Natural Sciences and Engineering Research  
 757 Council of Canada (NSERC) grant RGPIN-2020-04331.

## 759 References

- 760 Alexander, S., T. Coleman, and Y. Li (2006). Minimizing CVaR and VaR for a portfolio of derivatives. *Journal of*  
 761 *Banking and Finance* 30, 583–605.
- 762 Anarkulova, A., S. Cederburg, and M. S. O’Doherty (2022). Stocks for the long run? Evidence from a broad sample of  
 763 developed markets. *Journal of Financial Economics* 143:1, 409–433.
- 764 Bachouch, A., C. Huré, N. Langrené, and H. Pham (2022). Deep neural networks algorithms for stochastic control  
 765 problems on finite horizon: Numerical applications. *Methodology and Computing in Applied Probability* 24, 143–178.
- 766 Basak, S. and G. Chabakauri (2010). Dynamic mean-variance asset allocation. *Review of Financial Studies* 23, 2970–3016.
- 767 Beck, C., A. Jentzen, and B. Kuckuck (2022). Full error analysis for the training of deep neural networks. *Infinite*  
 768 *dimensional analysis, quantum probability and related topics* 25(2).

769 Bernard, C. and S. Vanduffel (2014). Mean-variance optimal portfolios in the presence of a benchmark with applications  
770 to fraud detection. *European Journal of Operational Research* 234, 469–480.

771 Bjork, T., M. Khapko, and A. Murgoci (2017). On time-inconsistent stochastic control in continuous time. *Finance and*  
772 *Stochastics* 21, 331–360.

773 Bjork, T., M. Khapko, and A. Murgoci (2021). *Time-inconsistent control theory with finance applications*. Springer  
774 Finance.

775 Bjork, T. and A. Murgoci (2010). A general theory of Markovian time inconsistent stochastic control problems. *Working*  
776 *paper* .

777 Bjork, T. and A. Murgoci (2014). A theory of Markovian time-inconsistent stochastic control in discrete time. *Finance*  
778 *and Stochastics* 18, 545–592.

779 Bodie, Z., A. Kane, and A. J. Marcus (2014). *Investments*. McGraw Hill New York, 10th edition edition.

780 Buehler, H., L. Gonon, J. Teichmann, and B. Wood (2019). Deep hedging. *Quantitative Finance* 19(8), 1271–1291.

781 Cavaglia, S., L. Scott, K. Blay, and S. Hixon (2022). Multi-asset class factor premia: A strategic asset allocation  
782 perspective. *The Journal of Portfolio Management* 48:9, 14–32.

783 Cogneau, P. and V. Zakalmouline (2013). Block bootstrap methods and the choice of stocks for the long run. *Quantitative*  
784 *Finance* 13:9, 1443–1457.

785 Dang, D. and P. Forsyth (2016). Better than pre-commitment mean-variance portfolio allocation strategies: A semi-self-  
786 financing Hamilton–Jacobi–Bellman equation approach. *European Journal of Operational Research* 250:1, 827–841.

787 Dichtl, H., W. Drobetz, and M. Wambach (2016). Testing rebalancing strategies for stock-bond portfolios across different  
788 asset allocations. *Applied Economics* 48, 772–788.

789 Dixon, M. F., I. Halperin, and P. Bilokon (2020). *Machine learning in finance*. Springer International Publishing.

790 Fama, E. and K. French (2015). A five-factor asset pricing model. *Journal of Financial Economics* 116(1), 1–22.

791 Fama, E. F. and K. R. French (1992). The cross-section of expected stock returns. *Journal of Finance* 47, 427–465.

792 Fernández-Villaverde, J., G. Nuño, G. Sorg-Langhans, and M. Vogler (2020). Solving high-dimensional dynamic pro-  
793 gramming problems using deep learning. *Working paper* .

794 Forsyth, P. (2020). Multiperiod mean conditional value at risk asset allocation: Is it advantageous to be time consistent?  
795 *SIAM Journal on Financial Mathematics* 11(2), 358–384.

796 Forsyth, P., J. Kennedy, S. Tse, and H. Windcliff (2011). Optimal trade execution: A mean quadratic variation approach.  
797 *Journal of Economic Dynamics and Control* 36:12, 1971–1991.

798 Forsyth, P. and K. Vetzal (2017). Dynamic mean variance asset allocation: Tests for robustness. *International Journal*  
799 *of Financial Engineering* 4:2. 1750021 (electronic).

800 Forsyth, P., K. Vetzal, and G. Westmacott (2019). Management of portfolio depletion risk through optimal life cycle  
801 asset allocation. *North American Actuarial Journal* 23(3), 447–468.

802 Forsyth, P. A. (2022). A stochastic control approach to defined contribution plan decumulation: The nastiest, hardest  
803 problem in finance. *North American Actuarial Journal* 26:2, 227–252.

804 Forsyth, P. A., P. M. Van Staden, and Y. Li (2023). Beating a constant weight benchmark: easier done than said.  
805 *International Journal of Theoretical and Applied Finance* Paper 350001 (electronic).

806 Forsyth, P. A. and K. R. Vetzal (2022). Multi-period mean expected-shortfall strategies: Cut your losses and ride your  
807 gains. *Applied Mathematical Finance* 29:5, 402–438.

808 Funahashi, K.-I. (1989). On the approximate realization of continuous mappings by neural networks. *Neural Networks*  
809 2, 183–189.

810 Gao, B. and L. Pavel (2018). On the properties of the softmax function with application in game theory and reinforcement  
811 learning. *Working paper* ArXiv 1704.00805.

812 Gao, Z., Y. Gao, Y. Hu, Z. Jiang, and J. Su (2020). Application of deep q-network in portfolio management. In *2020*  
813 *5th IEEE International Conference on Big Data Analytics (ICBDA)*, pp. 268–275.

814 Goodfellow, I., Y. Bengio, and A. Courville (2016). *Deep learning*. MIT press.

815 Granzol, D., X. Wan, S. Albanie, and S. Roberts (2021). Iterative averaging in the quest for best test error. *Working*  
816 *paper* .

817 Han, J., A. Jentzen, and E. Weinan (2018). Solving high-dimensional partial differential equations using deep learning.  
818 *PNAS* 115(34), 8505–8510.

819 Han, J. and E. Weinan (2016). Deep learning approximation for stochastic control problems. *NIPS Deep Reinforcement*  
820 *Learning Workshop* .

821 Henry-Labordère, P. (2017). Deep primal-dual algorithm for BSDEs: Application of machine learning to CVA and IM.  
822 *Working paper* .

823 Homer, S. and R. Sylla (2015). *A History of Interest Rates*. New York: Wiley.

824 Hornik, K. (1991). Approximation capabilities of multilayer feedforward networks. *Neural Networks* 4, 251–257.

825 Hornik, K., M. Stinchcombe, and H. White (1989). Multilayer feedforward networks are universal approximators. *Neural*  
826 *Networks* 2, 359–366.

- 827 Hu, R. and M. Laurière (2023). Recent developments in machine learning methods for stochastic control and games.  
828 *Working paper* .
- 829 Huré, C., H. Pham, A. Bachouch, and N. Langrené (2021). Deep neural networks algorithms for stochastic control  
830 problems on finite horizon: Convergence analysis. *SIAM Journal on Numerical Analysis* 59(1).
- 831 Jentzen, A., B. Kuckuck, A. Neufeld, and P. von Wurstemberger (2021). Strong error analysis for stochastic gradient  
832 descent optimization algorithms. *IMA Journal of Numerical Analysis* 41(1), 455–492.
- 833 Jin, H. Q., J. A. Yan, and X. Y. Zhou (2005). Continuous-time mean-risk portfolio selection. *Annales Henri Poincaré*  
834 18, 171–183.
- 835 Kingma, D. P. and J. L. Ba (2015). Adam: A method for stochastic optimization. *Published as a conference paper at*  
836 *ICLR 2015* .
- 837 Kou, S. G. (2002). A jump-diffusion model for option pricing. *Management Science* 48(8), 1086–1101.
- 838 Kratsios, A. and E. Bilokopytov (2020). Non-euclidean universal approximation. *Proceedings of the 34th Conference on*  
839 *Neural Information Processing Systems (NeurIPS 2020)*.
- 840 Leshno, M., V. Y. Lin, A. Pinkus, and S. Schocken (1993). Multilayer feedforward networks with a nonpolynomial  
841 activation function can approximate any function. *Neural Networks* 6, 861–867.
- 842 Li, D. and W.-L. Ng (2000). Optimal dynamic portfolio selection: multi period mean variance formulation. *Mathematical*  
843 *Finance* 10, 387–406.
- 844 Li, Y. and P. Forsyth (2019). A data-driven neural network approach to optimal asset allocation for target based defined  
845 contribution pension plans. *Insurance: Mathematics and Economics* 86, 189–204.
- 846 Li, Z., K. H. Tsang, and H. Y. Wong (2020). Lasso-based simulation for high-dimensional multi-period portfolio opti-  
847 mization. *IMA Journal of Management Mathematics* 31(3), 257–280.
- 848 Lucarelli, G. and M. Borrotti (2020). A deep q-learning portfolio management framework for the cryptocurrency market.  
849 *Neural Computing and Applications* 32(23), 17229–17244.
- 850 Merton, R. (1976). Option pricing when underlying stock returns are discontinuous. *Journal of Financial Economics* 3,  
851 125–144.
- 852 Miculescu, R. (2000). Approximation of continuous functions by Lipschitz functions. *Real Analysis Exchange* 26(1),  
853 449–452.
- 854 Miller, C. and I. Yang (2017). Optimal control of conditional value-at-risk in continuous time. *SIAM Journal on Control*  
855 *and Optimization* 55(2), 856–884.
- 856 Mucke, N., G. Neu, and L. Rosasco (2019). Beating SGD saturation with tail-averaging and minibatching. *33rd*  
857 *Conference on Neural Information Processing Systems (NeurIPS 2019)* .
- 858 Neu, G. and L. Rosasco (2018). Iterate averaging as regularization for stochastic gradient descent. *Proceedings of Machine*  
859 *Learning Research, 31st Annual Conference on Learning Theory* 75, 1–21.
- 860 Ni, C., Y. Li, P. Forsyth, and R. Carroll (2022). Optimal asset allocation for outperforming a stochastic benchmark  
861 target. *Quantitative Finance* 22:9, 1595–1626.
- 862 Oksendal, B. and A. Sulem (2019). *Applied Stochastic Control of Jump Diffusions*. Springer, 3rd edition.
- 863 Park, H., M. K. Sim, and D. G. Choi (2020). An intelligent financial portfolio trading strategy using deep q-learning.  
864 *Expert Systems with Applications* 158.
- 865 Politis, D. and J. Romano (1994). The stationary bootstrap. *Journal of the American Statistical Association* 89,  
866 1303–1313.
- 867 Polyak, B. T. and A. B. Juditsky (1992). Acceleration of stochastic approximation by averaging. *SIAM Journal on*  
868 *Control and Optimization* 30(4), 838–855.
- 869 Powell, W. (2023). A universal framework for sequential decision problems. *OR/MS Today* February. <https://tinyurl.com/PowellORMSfeature/>.
- 871 Reppen, A. M. and H. M. Soner (2023). Deep empirical risk minimization in finance: looking into the future. *Mathematical*  
872 *Finance* 33(1), 116–145.
- 873 Reppen, A. M., H. M. Soner, and V. Tissot-Daguette (2023). Deep stochastic optimization in finance. *Digital Finance*  
874 5, 91–111.
- 875 Rockafellar, R. and S. Uryasev (2002). Conditional value-at-risk for general loss distributions. *Journal of Banking and*  
876 *Finance* 26:7, 1443–1471.
- 877 Scott, L. and S. Cavaglia (2017). A wealth management perspective on factor premia and the value of downside protection.  
878 *The Journal of Portfolio Management* 43:3, 1–9.
- 879 Shapiro, A. and Y. Wardi (1996). Convergence analysis of gradient descent stochastic algorithms. *Journal of Optimization*  
880 *Theory and Applications* 91(2).
- 881 Simonian, J. and A. Martirosyan (2022). Sharpe parity redux. *The Journal of Portfolio Management* 48:9, 183–193.
- 882 Sonoda, S. and N. Murata (2017). Neural network with unbounded activation functions is universal approximator.  
883 *Applied and Computational Harmonic Analysis* 43, 233–268.

884 Strub, M., D. Li, and X. Cui (2019a). An enhanced mean-variance framework for robo-advising applications. SSRN  
885 3302111.

886 Strub, M. S., D. Li, X. Cui, and J. Gao (2019b). Discrete-time mean-CVaR portfolio selection and time-consistency  
887 induced term structure of the CVaR. *Journal of Economic Dynamics and Control* 108(103751).

888 Tsang, K. H. and H. Y. Wong (2020). Deep-learning solution to portfolio selection with serially dependent returns. *SIAM*  
889 *Journal on Financial Mathematics* 11(2), 593–619.

890 Tse, S., P. Forsyth, J. Kennedy, and H. Windcliff (2013). Comparison between the mean-variance optimal and the  
891 mean-quadratic-variation optimal trading strategies. *Applied Mathematical Finance* 20(5), 415–449.

892 Van Heeswijk, W. and H. L. Poutré (2019). Approximate dynamic programming with neural networks in linear discrete  
893 action spaces approximate dynamic programming with neural networks in linear discrete action spaces. *Working paper*  
894 .

895 Van Staden, P. M., P. A. Forsyth, and Y. Li (2023). Beating a benchmark: dynamic programming may not be the right  
896 numerical approach. *SIAM Journal on Financial Mathematics* 14(2).

897 Van Staden, P. M., P. A. Forsyth, and Y. Li (2024). Across-time risk-aware strategies for outperforming a benchmark.  
898 *European Journal of Operational Research* 313(2), 776–800.

899 Vigna, E. (2014). On efficiency of mean-variance based portfolio selection in defined contribution pension schemes.  
900 *Quantitative Finance* 14(2), 237–258.

901 Vigna, E. (2020). On time consistency for mean-variance portfolio selection. *International Journal of Theoretical and*  
902 *Applied Finance* 23(6).

903 Vigna, E. (2022). Tail optimality and preferences consistency for intertemporal optimization problems. *SIAM Journal*  
904 *on Financial Mathematics* 13(1).

905 Wang, R. and D. P. Foster (2020). What are the statistical limits of offline RL with linear function approximation?  
906 *Working paper* .

907 Yoon, J., D. Jarrett, and M. Van der Schaar (2019). Time-series generative adversarial networks. *33rd Conference*  
908 *on Neural Information Processing Systems (NeurIPS 2019)* [https://proceedings.neurips.cc/paper/2019/file/  
909 c9efe5f26cd17ba6216bbe2a7d26d490-Paper.pdf](https://proceedings.neurips.cc/paper/2019/file/c9efe5f26cd17ba6216bbe2a7d26d490-Paper.pdf).

910 Zhou, X. and D. Li (2000). Continuous time mean variance portfolio selection: a stochastic LQ framework. *Applied*  
911 *Mathematics and Optimization* 42, 19–33.

912 Zweng, Y. and Z. Li (2011). Asset liability management under benchmark and mean-variance criteria in a jump diffusion  
913 market. *Journal of Systems Science and Complexity* 24, 317–327.

## 914 Appendix A: NN approach: technical details and analytical results

915 In this appendix, additional analytical results, relating to the convergence analysis presented in Section 5, are  
916 presented.

### 917 A.1: NN structural assumptions

918 In this section, we discuss the NN structural assumptions. First, we introduce the necessary notation - for a  
919 more detailed treatment of NNs, see for example Goodfellow et al. (2016). Consider a fully-connected, feed-  
920 forward NN  $\mathbf{f}_n$  with  $\mathcal{L}^h \geq 1$  hidden layers. The NN layers are indexed by  $\ell \in \{0, \dots, \mathcal{L}\}$ , where  $\ell = 0$  and  
921  $\ell = \mathcal{L}^h + 1 \equiv \mathcal{L}$  denote the input and output layers, respectively. Let  $\eta_{n,\ell} \in \mathbb{N}$  denote the number of nodes  
922 in layer  $\ell$  of  $\mathbf{f}_n$ . With the exception of the input layer, each layer  $\ell \in \{1, \dots, \mathcal{L}\}$  is associated with a weights  
923 matrix  $\mathbf{x}_n^{[\ell]} \in \mathbb{R}^{\eta_{n,\ell} \times \eta_{n,\ell-1}}$  into the layer, an optional bias vector  $\mathbf{b}_n^{[\ell]} \in \mathbb{R}^{\eta_{n,\ell}}$ , as well as an activation function  
924  $\mathbf{a}_n^{[\ell]} : \mathbb{R}^{\eta_{n,\ell}} \rightarrow \mathbb{R}^{\eta_{n,\ell}}$  which is applied to the weighted inputs into the layer.

925 The parameter vector of the NN  $\mathbf{f}_n$ , which consists of all weights and biases, is denoted by  $\boldsymbol{\theta}_n \in \mathbb{R}^{\nu_n}$ , where  
926  $\nu_n \in \mathbb{N}$  denotes the total number of weights and biases. In other words, the weights matrices  $\{\mathbf{x}_n^{[\ell]} : \ell = 1, \dots, \mathcal{L}\}$   
927 and optional bias vectors  $\{\mathbf{b}_n^{[\ell]} : \ell = 1, \dots, \mathcal{L}\}$  are transformed into a single vector  $\boldsymbol{\theta}_n = (\theta_1, \dots, \theta_{\nu_n})$ , where each  
928  $\theta_{n,i} \in \boldsymbol{\theta}_n$  can be uniquely mapped to a single weight or bias in some layer.

929 Note that no activation function is applied at the input layer ( $\ell = 0$ ), so that the  $\eta_0 \equiv \eta_{n,0}$  output values of  
930 the input layer corresponds to feature (input) vector of the NN, which will be denoted by  $\boldsymbol{\phi} \in \mathbb{R}^{\eta_0}$ . Recalling  
931 that  $\eta_{\mathcal{L}} \equiv \eta_{n,\mathcal{L}}$  is the number of nodes in the output layer ( $\ell = \mathcal{L}$ ) and setting the bias vectors  $\mathbf{b}_n^{[\mathcal{L}]} \equiv \mathbf{0}$  for  
932 convenience, the NN can therefore be written as a single function  $\mathbf{f}_n(\boldsymbol{\phi}; \boldsymbol{\theta}_n) : \mathbb{R}^{\eta_0} \rightarrow \mathbb{R}^{\eta_{\mathcal{L}}}$ , where

$$933 \quad \mathbf{f}_n(\boldsymbol{\phi}; \boldsymbol{\theta}_n) := (f_{n,1}(\boldsymbol{\phi}; \boldsymbol{\theta}_n), \dots, f_{n,\eta_{\mathcal{L}}}(\boldsymbol{\phi}; \boldsymbol{\theta}_n)), \quad \boldsymbol{\phi} \in \mathbb{R}^{\eta_0}, \boldsymbol{\theta}_n \in \mathbb{R}^{\nu_n} \quad (\text{A.1})$$

934 We highlight that the output of the  $i$ th node in the output layer is given by  $f_{n,i}(\boldsymbol{\phi}; \boldsymbol{\theta}_n) = \mathbf{a}_{n,i}^{[\mathcal{L}]}$ .

935 Given this standard fully-connected, feedforward NN formulation, we introduce the following NN structural  
 936 assumption.

937 **Assumption A.1.** (NN structure) Let  $\mathbf{f}_n(\cdot; \boldsymbol{\theta}_n)$ ,  $n \in \mathbb{N}$ , be a sequence of fully-connected feedforward neural  
 938 networks, and let  $\bar{h}(n)$ ,  $n \in \mathbb{N}$  be a monotonically increasing sequence (i.e.  $\bar{h}(n) < \bar{h}(n+1)$ ,  $\forall n \in \mathbb{N}$ ) such that  
 939  $\lim_{n \rightarrow \infty} \bar{h}(n) = \infty$ . For each  $n \in \mathbb{N}$ , the NN  $\mathbf{f}_n$  is constructed to satisfy the following structural assumptions.

940 (i) The number of hidden layers  $\mathcal{L}^h \geq 1$  ( $\mathcal{L}^h \in \mathbb{N}$ ) remains fixed for all  $n \in \mathbb{N}$ . For notational simplicity, we  
 941 assume that each of the  $\mathcal{L}^h$  hidden layers of the NN  $\mathbf{f}_n$  has the same number  $\bar{h}(n)$  of hidden nodes,

$$942 \quad \eta_{n,\ell} \equiv \bar{h}(n), \quad \forall \ell = 1, \dots, \mathcal{L} - 1, \quad \text{for some } \bar{h}(n) \in \mathbb{N}. \quad (\text{A.2})$$

943 (ii) For convenience, we assume that the sigmoid activation function  $\sigma^h$  is applied at each hidden node,

$$944 \quad \sigma^h(y) = \frac{1}{1 + e^{-y}} \equiv \mathbf{a}_{n,i}^{[\ell]}(y), \quad \text{where } y = \left( \sum_{k=1}^{\eta_{n,\ell-1}} x_{n,ik}^{[\ell]} \mathbf{a}_{n,k}^{[\ell-1]} \right) + b_{n,i}^{[\ell]}, \quad (\text{A.3})$$

945 for all  $\ell = 1, \dots, \mathcal{L}^h$  and  $i = 1, \dots, \bar{h}(n)$ . Note that in principle, any of the popular activation functions can  
 946 be used instead of (A.3), with minor modifications to the theoretical analysis presented in this paper.

947 (iii) The NN  $\mathbf{f}_n$  has  $\eta_0 = \eta_X + 1 \equiv \eta_{n,0}$  input nodes (i.e. the number of input nodes are independent of  $n \in \mathbb{N}$ ),  
 948 with feature (input) vectors  $\boldsymbol{\phi} \in \mathbb{R}^{\eta_0}$  of the form

$$949 \quad \boldsymbol{\phi} := \boldsymbol{\phi}(t) := (t, \mathbf{X}(t)) \in \mathcal{D}_{\boldsymbol{\phi}} \subseteq \mathbb{R}^{\eta_X + 1}, \quad \text{with } \mathbf{X}(t) = (W(t^+), \hat{\mathbf{X}}(t)), \quad (\text{A.4})$$

950 where  $W(t^+)$  denotes the wealth available for investment at time  $t$  after any contributions to the portfolio  
 951 at time  $t$ , while  $\hat{\mathbf{X}}(t)$  denotes a vector of additional information taken into account by the investment  
 952 strategy. We emphasize that (A.4) clarifies that at time  $t \in [t_0, T]$ , at least time  $t$  itself and  $W(t^+)$  are  
 953 always assumed to be inputs into the NN.

954 (iv) The NN  $\mathbf{f}_n$  has  $N_a = \eta_{n,\mathcal{L}}$  output nodes (i.e. the number of output nodes are independent of  $n \in \mathbb{N}$ ), with  
 955 the output of node  $i$ , denoted by  $f_{n,i}(\boldsymbol{\phi}(t); \boldsymbol{\theta}_n)$ , being associated with the proportion of available wealth  
 956  $W(t^+)$  invested in asset  $i \in \{1, \dots, N_a\}$  after rebalancing the portfolio at time  $t$ .

957 (v) The output layer ( $\ell = \mathcal{L} = \mathcal{L}^h + 1$ ) of each NN  $\mathbf{f}_n$  uses the softmax activation function (see for example  
 958 Gao and Pavel (2018)). Therefore we have  $\mathbf{a}_n^{[\mathcal{L}]} = \boldsymbol{\psi} : \mathbb{R}^{N_a} \rightarrow \mathbb{R}^{N_a}$ , where the  $i$ th component of  $\boldsymbol{\psi} =$   
 959  $(\psi_i : i = 1, \dots, N_a)$  is given by

$$960 \quad \psi_i = \mathbf{a}_{n,i}^{[\mathcal{L}]} = \frac{\exp\{z_{n,i}^{[\mathcal{L}]}\}}{\sum_{m=1}^{N_a} \exp\{z_{n,m}^{[\mathcal{L}]}\}}, \quad \text{where } z_{n,i}^{[\mathcal{L}]} = \sum_{k=1}^{N_a} x_{n,ik}^{[\mathcal{L}]} \mathbf{a}_{n,k}^{[\mathcal{L}-1]} + b_{n,i}^{[\mathcal{L}]}, \quad i = 1, \dots, N_a. \quad (\text{A.5})$$

961 For a given  $n \in \mathbb{N}$ , we define the set  $\mathcal{N}_n$  as the set of all neural networks satisfying Assumption (A.1),

$$962 \quad \mathcal{N}_n = \{ \mathbf{f}_n : \mathcal{D}_{\boldsymbol{\phi}} \rightarrow \mathcal{Z} \mid \mathbf{f}_n(\cdot; \boldsymbol{\theta}_n) \text{ satisfies Assumption A.1 with } \bar{h}(n) \text{ nodes in each hidden layer} \}. \quad (\text{A.6})$$

963 In other words, each  $\mathbf{f}_n(\cdot; \boldsymbol{\theta}_n) \in \mathcal{N}_n$  has the same number of hidden nodes  $\bar{h}(n)$  in each hidden layer, but a  
 964 potentially different parameter vector  $\boldsymbol{\theta}_n$  (i.e. different values associated with the weights and biases).

965 We make the following observations regarding Assumption A.1:

- 966 • Any NN constructed to satisfy Assumption A.1 will, for any input vector  $\boldsymbol{\phi}(t)$ , automatically generate  
 967 an output in the set  $\mathcal{Z}$ , hence the definition (A.6) noting that  $\mathbf{f}_n : \mathcal{D}_{\boldsymbol{\phi}} \rightarrow \mathcal{Z}$ . In other words, the given  
 968 constraints are automatically satisfied. However, different sets of constraints simply requires modifications  
 969 to the output activation, or post-processing of NN outputs, without affecting the technical results.
- 970 • Note that further assumptions regarding the rate of at which the sequence  $\bar{h}(n)$  increases relative to that  
 971 of the sequence  $\{n\}_{n \in \mathbb{N}}$  will be introduced in the convergence analysis of Section 5 (see Assumption A.4).



- In practical applications, it is not necessary to consider a sequence of NNs; instead, we will use a single NN  $\mathbf{f}_{\tilde{n}}$  with  $\tilde{h}(\tilde{n})$  hidden nodes in each of the hidden layers to get a reasonable trade-off between accuracy and computational efficiency. However, we emphasize that any such  $\mathbf{f}_{\tilde{n}}$  is still constructed to satisfy Assumption A.1.

## A.2: Assumptions for convergence analysis

Assumption A.2 introduces the main assumptions used in rigorously justifying the approximation (4.8) and therefore to prove Theorem 5.1.

**Assumption A.2.** (*Convergence analysis: NN approximation to control*) To establish the validity of the NN approximation to the control, we make the following assumptions:

- (i) The optimal investment strategy (or control) satisfies Assumption 4.1.
- (ii) The functions  $F$  and  $G$  in the objective functional  $J(\mathbf{p}, \xi; t_0, w_0)$  (see (4.4)) are continuous, and  $\xi \rightarrow F(\cdot, \xi)$  and  $\xi \rightarrow G(\cdot, \cdot, \cdot, \xi)$  are convex for any admissible strategy  $\mathbf{p} \in C(\mathcal{D}_\phi, \mathcal{Z})$ . Note that in for example the Mean - Conditional Value-at-Risk problem (3.15) where there is an inner and outer optimization problem, this assumption is standard in computational settings (Forsyth (2020)).
- (iii) The NN approximation (4.8) of the investment strategy  $\mathbf{p} \in C(\mathcal{D}_\phi, \mathcal{Z})$  is implemented by a NN  $\mathbf{f}_n(\cdot; \boldsymbol{\theta}_n) \in \mathcal{N}_n$ , where  $\mathcal{N}_n$  is given by (A.6). In other words, each approximating NN in the sequence of NNs  $\mathbf{f}_n, n \in \mathbb{N}$  is constructed according to Assumption A.1.

Note that Assumption A.2(iii) specifically requires that Assumption A.1 is satisfied, so each  $\mathbf{f}_n, n \in \mathbb{N}$ , has  $\tilde{h}(n)$  nodes in each hidden layer, where we recall that the sequence  $\tilde{h}(n), n \in \mathbb{N}$ , is monotonically increasing and satisfies  $\tilde{h}(n) \rightarrow \infty$  as  $n \rightarrow \infty$ . However, we make no further assumptions yet regarding the form of  $n \rightarrow \tilde{h}(n)$ .

For ease of exposition, we introduce Assumption A.3 below. We emphasize that Assumption A.3 is purely for the sake of convenience, with Remark A.1 below discussing briefly how each component of Assumption A.3 can be relaxed with only minor (but tedious and notationally demanding) modifications to the subsequent proofs.

**Assumption A.3.** (*Convergence analysis: Assumptions for ease of exposition*) For convenience, we introduce the following assumptions which can be relaxed without difficulty, as discussed in Remark A.1 below.

- (i) We assume that the optimal control  $\mathbf{p}^*$  as per Assumption 4.1 is a function of time and wealth only, i.e.  $\mathbf{X}^*(t_m) = W^*(t_m^+)$  for each  $t_m \in \mathcal{T}$  in (4.2). As a result, we work with the minimal form of the NN feature vector satisfying Assumption A.1. Specifically, in the subsequent results we will always assume that  $\mathbf{X}(t) = W(t^+)$ , so that we will consider feature vectors (A.4) of the form

$$\phi(t) = (t, W(t^+; \boldsymbol{\theta}_n, \mathbf{Y})) \in \mathcal{D}_\phi \subseteq \mathbb{R}^2. \quad (\text{A.7})$$

- (ii) The wealth process with dynamics given by (4.10) remains bounded. In other words, we assume that there exists a value  $w_{max} > 0$  such that

$$0 \leq W(t; \boldsymbol{\theta}_n, \mathbf{Y}) \leq w_{max} \quad \text{a.s.} \quad \text{for all } t \in [t_0, T], \boldsymbol{\theta}_n \in \mathbb{R}^{\nu_n}, \quad (\text{A.8})$$

so that  $\mathcal{D}_\phi$  in (A.7) satisfies

$$\mathcal{D}_\phi = [t_0, T] \times [0, w_{max}]. \quad (\text{A.9})$$

The following remark discusses how Assumption A.3 can be relaxed.

**Remark A.1.** (Relaxing Assumption A.3) As noted above, Assumption A.3 has been introduced for ease of exposition. We therefore briefly describe how each element of element of Assumption A.3 can be relaxed without difficulty.

- (i) In the case where the state  $\mathbf{X}^*(t_m)$  depends on variables in addition to the portfolio wealth, for example historical returns or additional variables (see for example Forsyth (2020); Tsang and Wong (2020)), it is straightforward to incorporate these extra values without materially impacting the key aspects of the convergence analysis. However, it is essential that portfolio wealth is included in  $\mathbf{X}^*(t_m)$  as per Assumption 4.1.

1016 (ii) The assumption of bounded wealth (A.8) is clearly practical, in that while it is undoubtedly true that the  
 1017 entire wealth of the world is very large, it remains finite. However, from a theoretical perspective, the  
 1018 only reason we introduce (A.8) is to ensure that, given the minimal form of the feature vector (A.7), the  
 1019 controls take inputs in a compact domain (A.9). While boundedness assumptions can be relaxed without  
 1020 theoretical difficulty using straightforward localization arguments (see for example Huré et al. (2021);  
 1021 Tsang and Wong (2020)), this simply introduces yet further notational complexity without providing  
 1022 additional insights into the fundamental arguments underlying the subsequent proofs.

1023  $\square$

1024 In the convergence analysis of Step 2 of the proposed approach, namely the computational estimate of the  
 1025 optimal control obtained using (4.16), we need to introduce some additional assumptions (Assumption A.4  
 1026 below) since this step involves the training dataset  $\mathcal{Y}_n$  of the NN and numerical solution of problem (4.16).

1027 **Assumption A.4.** (*Convergence analysis: Computational estimate of optimal control*) We introduce the fol-  
 1028 lowing assumptions:

1029 (i) The training data set  $\mathcal{Y}_n = \{\mathbf{Y}^{(j)} : j \in \{1, \dots, n\}\}$  used for training the NN (see (4.13) and associated  
 1030 discussion) is constructed with independent joint asset return paths  $\mathbf{Y}^{(j)} \in \mathcal{Y}_n$ . As noted before, this does  
 1031 not assume that the joint asset returns along a given path are independent or serially independent.

1032 (ii) Number of nodes in each hidden layer  $\bar{h}(n), n \in \mathbb{N}$ : As  $n \rightarrow \infty$  ( $n \in \mathbb{N}$ ), in the case of one hidden layer  
 1033 ( $\mathcal{L}^h = 1$ ), we assume that  $\bar{h}(n) = o(n^{1/4})$ . For deeper NNs ( $\mathcal{L}^h > 1$ ), we assume that  $\bar{h}(n) = o(n^{1/6})$ .

1034 (iii) For each  $n \in \mathbb{N}$ , the optimization algorithm used in solving problem (4.16) attains the minimum  $(\hat{\boldsymbol{\theta}}_n^*, \hat{\xi}_n^*) \in$   
 1035  $\mathbb{R}^{\nu_n+1}$  corresponding to a given training data set  $\mathcal{Y}_n$ .

1036 Since stochastic gradient descent (SGD) is used in training the NN, Assumption A.4(iii) is very strong;  
 1037 however, it is a standard assumption in convergence analyses in the literature (see for example Huré et al.  
 1038 (2021); Tsang and Wong (2020)) in order to focus on the key aspects of a proposed approach. For detailed  
 1039 treatments of theoretical aspects regarding optimization errors (i.e. the differences between the attained values  
 1040 and the true minima) arising when training NNs, the reader is referred to for example Beck et al. (2022); Jentzen  
 1041 et al. (2021). Note that Assumption A.4(ii), which can also be found in Tsang and Wong (2020), is used to  
 1042 establish a version of the law of large numbers that is applicable to our setting.

1043 **Remark A.2** (Increase in number of training samples as  $\bar{h}$  increases). Informally, Assumption A.4(ii) requires  
 1044 that the number of training samples  $n$  grows faster than  $O(\bar{h}^4)$  for  $\mathcal{L}^h = 1$  and  $O(\bar{h}^6)$  for  $\mathcal{L}^h > 1$ , where  $\bar{h}$   
 1045 is the number of nodes in each hidden layer. Since we require a large  $\bar{h}$  (number of nodes in each layer) for  
 1046 good function approximation, this would suggest that convergence in terms of both function approximation  
 1047 and sampling error requires a very large number of sample paths. This would appear to result in a barrier  
 1048 to obtaining accurate results, for practical numbers of samples. However, our numerical examples seem to  
 1049 produce solutions with reasonable errors, hence the requirements of Assumption A.4(ii) are probably not sharp.  
 1050 Regardless, we can certainly expect that the number of samples should be significantly increased as we increase  
 1051  $\bar{h}$ .

### 1052 A.3: Proof of Theorem 5.1

1053 Before presenting the proof of Theorem 5.1, we first prove some auxiliary results that are preliminary require-  
 1054 ments for the proof.

1055 We start with Lemma A.5, which combines and applies selected universal approximation results to our  
 1056 setting. The use of the notation  $\mathbf{f}_n^*(\cdot, \boldsymbol{\theta}_n^*) \in \mathcal{N}_n$  in Lemma A.5, which has been defined in Subsection 4.1 as  
 1057 the NN using the optimal parameter vector consistent with problem (4.11)-(4.12), will become clear in the  
 1058 subsequent results.

1059 **Lemma A.5.** (*Convergence to optimal control*) Suppose that Assumption A.2 and Assumption A.3 hold. As  
 1060 per (4.2), let  $\mathbf{p}^* = (p_i^* : i = 1, \dots, N_a) \in C(\mathcal{D}_\phi, \mathcal{Z})$  denote the optimal control associated with problem (4.6).  
 1061 Then there exists a sequence of neural networks,  $\mathbf{f}_n^* \in \mathcal{N}_n$ ,  $n \in \mathbb{N}$ , where each  $\mathbf{f}_n^* = (f_{n,i}^* : i = 1, \dots, N_a)$  has  
 1062 parameter vector  $\boldsymbol{\theta}_n^* \in \mathbb{R}^{\nu_n}$ , such that

$$1063 \lim_{n \rightarrow \infty} \sup_{\phi \in \mathcal{D}_\phi} |f_{n,i}^*(\phi; \boldsymbol{\theta}_n^*) - p_i^*(\phi)| = 0, \quad \forall i = 1, \dots, N_a, \quad (\text{A.10})$$

1064 *Proof.* For ease of reference, recall that we have defined  $\mathcal{N}_n$  as the set of NNs with  $\bar{h}(n)$  hidden nodes in each  
 1065 of the (fixed number of)  $\mathcal{L}^h \geq 1$  hidden layers, constructed according to Assumption A.1,

$$1066 \quad \mathcal{N}_n = \{ \mathbf{f}_n : \mathcal{D}_\phi \rightarrow \mathcal{Z} \mid \mathbf{f}_n(\cdot; \boldsymbol{\theta}_n) \text{ satisfies Assumption A.1 with } \bar{h}(n) \text{ nodes in each hidden layer} \}. \quad (\text{A.11})$$

1067 Consider another sequence of NNs,  $\overset{\circ}{\mathbf{f}}_n, n \in \mathbb{N}$ , where each  $\overset{\circ}{\mathbf{f}}_n : \mathcal{D}_\phi \rightarrow \mathbb{R}^{N_a}$  is structurally identical to the  
 1068 corresponding  $\mathbf{f}_n \in \mathcal{N}_n$  in terms of Assumption A.1, *except* that  $\overset{\circ}{\mathbf{f}}_n$  uses the identity as the (linear) output  
 1069 activation function. Specifically, we assume that  $\overset{\circ}{\mathbf{f}}_n$  does not apply the activation (A.1) at its output layer, but  
 1070 instead replaces (A.1) with  $\overset{\circ}{\mathbf{a}}_n^{[\mathcal{L}]} = \left( \overset{\circ}{\mathbf{a}}_{n,i}^{[\mathcal{L}]} : i = 1, \dots, N_a \right) : \mathbb{R}^{N_a} \rightarrow \mathbb{R}^{N_a}$  where

$$1071 \quad \overset{\circ}{\mathbf{a}}_{n,i}^{[\mathcal{L}]} \left( \mathbf{z}_n^{[\mathcal{L}]} \right) = z_{n,i}^{[\mathcal{L}]} = \sum_{k=1}^{N_a} x_{n,ik}^{[\mathcal{L}]} \mathbf{a}_{n,k}^{[\mathcal{L}-1]} + b_{n,i}^{[\mathcal{L}]}, \quad \forall i = 1, \dots, N_a. \quad (\text{A.12})$$

1072 For any given  $n \in \mathbb{N}$ , the relationship between  $\mathbf{f}_n$  and  $\overset{\circ}{\mathbf{f}}_n$  are illustrated in Figure A.1. Note that the entire  
 1073 parameter vector  $\boldsymbol{\theta}_n$  of  $\mathbf{f}_n$  is inherited by  $\overset{\circ}{\mathbf{f}}_n$ , since all the weights, biases, and hidden layers and nodes of  $\overset{\circ}{\mathbf{f}}_n$   
 1074 and  $\mathbf{f}_n$  are identical. As a result, we define the set  $\overset{\circ}{\mathcal{N}}_n$

$$1075 \quad \overset{\circ}{\mathcal{N}}_n = \left\{ \overset{\circ}{\mathbf{f}}_n : \mathcal{D}_\phi \rightarrow \mathbb{R}^{N_a} \mid \overset{\circ}{\mathbf{f}}_n(\cdot; \boldsymbol{\theta}_n) \text{ satisfies Assumption A.1, except} \right. \\
 1076 \quad \left. \text{output activation (A.5) is replaced by (A.12).} \right\}, \quad (\text{A.13})$$

1077 where we note that the outputs of  $\overset{\circ}{\mathbf{f}}_n$  take values which are no longer in  $\mathcal{Z} \subset \mathbb{R}^{N_a}$ , but instead merely in  $\mathbb{R}^{N_a}$ .  
 1078 The main benefit of working with  $\overset{\circ}{\mathbf{f}}_n \in \overset{\circ}{\mathcal{N}}_n$  instead of  $\mathbf{f}_n \in \mathcal{N}_n$ , is that the linear output layer (A.12) means  
 1079 that each  $\overset{\circ}{\mathbf{f}}_n \in \overset{\circ}{\mathcal{N}}_n$  is in the standard form used by most universal approximation theorems for NNs (see for  
 1080 example Funahashi (1989); Hornik (1991); Hornik et al. (1989); Leshno et al. (1993)).

1081 Recalling for convenience the definition of the softmax function  $\boldsymbol{\psi} = (\psi_i : i = 1, \dots, N_a) : \mathbb{R}^{N_a} \rightarrow \mathbb{R}^{N_a}$  in  
 1082 (A.5),

$$1083 \quad \psi_i(\mathbf{y}) = \frac{\exp\{y_i\}}{\sum_{j=1}^{N_a} \exp\{y_j\}}, \quad \forall \mathbf{y} = (y_i : i = 1, \dots, N_a) \in \mathbb{R}^{N_a}, \quad (\text{A.14})$$

we therefore observe that for any  $n \in \mathbb{N}$ , the NN  $\mathbf{f}_n(\cdot; \boldsymbol{\theta}_n) \in \mathcal{N}_n$  can be expressed as a transformation of the  
 corresponding NN  $\overset{\circ}{\mathbf{f}}_n(\cdot; \boldsymbol{\theta}_n) \in \overset{\circ}{\mathcal{N}}_n$ , provided both NNs use the same parameter vector  $\boldsymbol{\theta}_n \in \mathbb{R}^{\nu_n}$ :

$$\mathbf{f}_n(\cdot; \boldsymbol{\theta}_n) = \boldsymbol{\psi} \circ \overset{\circ}{\mathbf{f}}_n(\cdot; \boldsymbol{\theta}_n), \quad \text{where } \overset{\circ}{\mathbf{f}}_n(\cdot; \boldsymbol{\theta}_n) \in \overset{\circ}{\mathcal{N}}_n. \quad (\text{A.15})$$

1084 As per Assumption A.1, recall that  $\bar{h}(n), n \in \mathbb{N}$  satisfies  $\bar{h}(n) < \bar{h}(n+1), \forall n \in \mathbb{N}$  such that  $\lim_{n \rightarrow \infty} \bar{h}(n) =$   
 1085  $\infty$ . Inspired by the notation of Hornik (1991), we define the sets  $\mathcal{N}_\infty$  and  $\overset{\circ}{\mathcal{N}}_\infty$  as the sets of NNs constructed  
 1086 according to (A.11) and (A.13), respectively, but with an arbitrarily large number of hidden nodes,

$$1087 \quad \mathcal{N}_\infty = \bigcup_{n \in \mathbb{N}} \mathcal{N}_n, \quad \text{and} \quad \overset{\circ}{\mathcal{N}}_\infty = \bigcup_{n \in \mathbb{N}} \overset{\circ}{\mathcal{N}}_n. \quad (\text{A.16})$$

1088 Since  $\mathcal{D}_\phi \subset \mathbb{R}^{\eta_x+1}$  is compact by (A.9) as per Assumption A.3 (note that this requirement can be relaxed  
 1089 without difficulty as discussed in Remark A.1), we know by the results of Hornik (1991); Hornik et al. (1989)  
 1090 that  $\overset{\circ}{\mathcal{N}}_\infty$  is uniformly dense in  $C(\mathcal{D}_\phi, \mathbb{R}^{N_a})$ . In other words, for any function  $\overset{\circ}{\mathbf{g}} = \left( \overset{\circ}{g}_i : i = 1, \dots, N_a \right) \in$   
 1091  $C(\mathcal{D}_\phi, \mathbb{R}^{N_a})$  and any  $\epsilon > 0$ , there exists a value of  $n = n_\epsilon$  sufficiently large such that the corresponding NN  
 1092  $\overset{\circ}{\mathbf{f}}_{n_\epsilon} = \left( \overset{\circ}{f}_{n_\epsilon,i} : i = 1, \dots, N_a \right) \in \overset{\circ}{\mathcal{N}}_{n_\epsilon}$  such that

$$1093 \quad \sup_{\boldsymbol{\phi} \in \mathcal{D}_\phi} \left| \overset{\circ}{f}_{n_\epsilon,i}(\boldsymbol{\phi}; \boldsymbol{\theta}_{n_\epsilon}) - \overset{\circ}{g}_i(\boldsymbol{\phi}) \right| < \epsilon, \quad \forall i = 1, \dots, N_a. \quad (\text{A.17})$$

1094 Note that (A.17) holds for any given number  $\mathcal{L}^h \geq 1$  of hidden layers (see for example Corollary 2.7 in Hornik  
 1095 et al. (1989)).

1096 Using the results of Gao and Pavel (2018), the softmax (A.14) is (Lipschitz) continuous and surjective,  
 1097 since  $\psi_i(\mathbf{y}) = \psi_i(\mathbf{y} + c)$  for any  $\mathbf{y} \in \mathbb{R}^{N_a}$  and  $c \in \mathbb{R}$ , where  $\mathbf{y} + c := (y_i + c : i = 1, \dots, N_a)$ . In addition, it has  
 1098 a continuous right-inverse; as an example, we can simply consider the function  $\overleftarrow{\psi}(\mathbf{z}) = (\log(z_i) : i = 1, \dots, N_a)$   
 1099 where each  $z_i \in (0, 1)$  and that  $\sum_i z_i = 1$ . Furthermore, by Assumption A.1, no activation function is applied  
 1100 at the input layer (i.e. the “input activation” is trivially injective and continuous). Using these properties of  
 1101 the input and output layers of any  $\mathbf{f}_n \in \mathcal{N}_n$  together with the results (A.15) and (A.17), we can conclude by  
 1102 the results of Kratsios and Bilokopytov (2020) that the set  $\mathcal{N}_\infty$  is uniformly dense in  $C(\mathcal{D}_\phi, \mathcal{Z})$ .

1103 Applying this result specifically to the optimal control  $\mathbf{p}^* \in C(\mathcal{D}_\phi, \mathcal{Z})$  as per Assumption 4.1, we can  
 1104 conclude that, for any  $\epsilon > 0$ , there exists a value  $n = n_\epsilon$  sufficiently large such that the corresponding NN  
 1105  $\mathbf{f}_{n_\epsilon}^*(\cdot; \boldsymbol{\theta}_{n_\epsilon}^*) \in \mathcal{N}_{n_\epsilon}$  satisfies

$$1106 \quad \sup_{\phi \in \mathcal{D}_\phi} |f_{n_\epsilon, i}^*(\phi; \boldsymbol{\theta}_{n_\epsilon}^*) - p_i^*(\phi)| < \epsilon, \quad \forall i = 1, \dots, N_a. \quad (\text{A.18})$$

1107 Note that the exact output of the NN  $\mathbf{f}_{n_\epsilon}^* \in \mathcal{N}_{n_\epsilon}$ , which we recall has  $\bar{h}(n_\epsilon)$  hidden nodes in each hidden layer,  
 1108 can be attained by a NN with  $\bar{h}(n_\epsilon + k)$ ,  $k \in \mathbb{N}$  hidden nodes, since we can always set the weights and biases  
 1109 corresponding to the additional  $\bar{h}(n_\epsilon + k) - \bar{h}(n_\epsilon)$  nodes identically to zero. In other words, (A.18) implies  
 1110 the existence of a sequence of NNs  $\mathbf{f}_n^*(\cdot; \boldsymbol{\theta}_n^*)$ ,  $n \in \mathbb{N}$ , where each  $\mathbf{f}_n^*(\cdot; \boldsymbol{\theta}_n^*) \in \mathcal{N}_n$ , such that for any  $\epsilon > 0$  and  
 1111 sufficiently large  $n_\epsilon \in \mathbb{N}$ , we have

$$1112 \quad \sup_{\phi \in \mathcal{D}_\phi} |f_{n, i}^*(\phi; \boldsymbol{\theta}_n^*) - p_i^*(\phi)| < \epsilon, \quad \forall n \geq n_\epsilon, i = 1, \dots, N_a, \quad (\text{A.19})$$

1113 completing the proof of (A.10). □

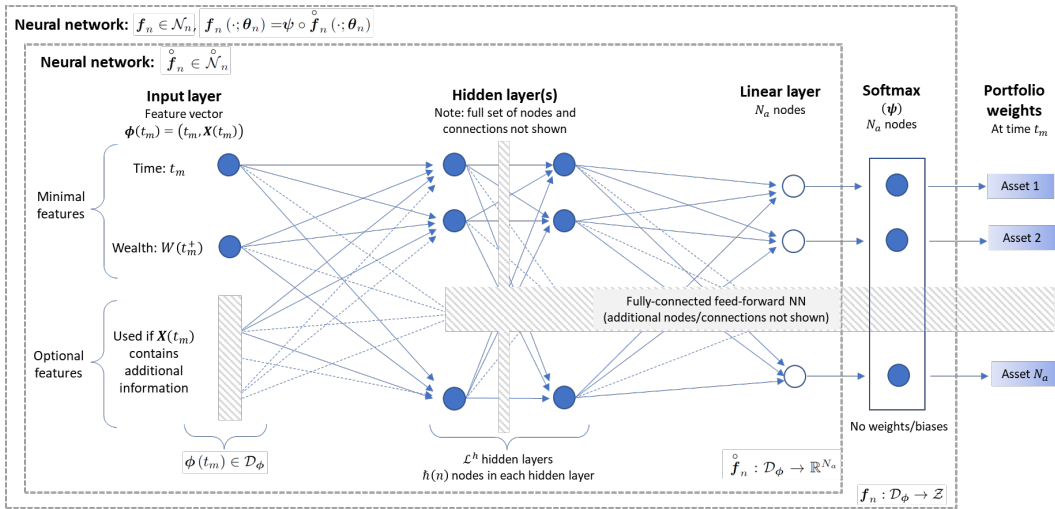


**Figure A.1:** Illustration of the interpretation of the NN  $\mathbf{f}_n(\cdot; \boldsymbol{\theta}_n)$  as a composition of the softmax  $\psi$  and the NN  $\mathbf{f}_n(\cdot; \boldsymbol{\theta}_n)$  as per equation (A.15).

1114 If Assumption 4.2 and Assumption A.3 are applicable, the wealth dynamics (4.5) using the optimal control  
 1115 is given by  
 1116

$$1117 \quad W^*(t_{m+1}^-; \mathbf{p}^*, \mathbf{Y}) = W^*(t_m^+; \mathbf{p}^*, \mathbf{Y}) \cdot \prod_{i=1}^{N_a} p_i^*(t_m, W^*(t_m^+; \mathbf{p}^*, \mathbf{Y})) \cdot Y_i(t_m), \quad t_m \in \mathcal{T}, \quad (\text{A.20})$$

where we recall that  $W^*(t_m^+; \mathbf{p}^*, \mathbf{Y}) = W^*(t_m^-; \mathbf{p}^*, \mathbf{Y}) + q(t_m)$ ,  $\mathbf{X}^*(t_m) = W^*(t_m^+; \mathbf{p}^*, \mathbf{Y})$  and  $W^*(t_{N_r b}^-) := W^*(T)$ . Furthermore, associated with every NN in the sequence  $\mathbf{f}_n^*(\cdot; \boldsymbol{\theta}_n^*) \in \mathcal{N}_n$  identified in Lemma A.5, we

have the corresponding wealth dynamics as per (4.10) that satisfies

$$W^*(t_{m+1}^-; \boldsymbol{\theta}_n^*, \mathbf{Y}) = W^*(t_m^+; \boldsymbol{\theta}_n^*, \mathbf{Y}) \cdot \sum_{i=1}^{N_a} f_{n,i}^*(t_m, W^*(t_m^+; \boldsymbol{\theta}_n^*, \mathbf{Y}); \boldsymbol{\theta}_n^*) \cdot Y_i(t_m), \quad t_m \in \mathcal{T}, n \in \mathbb{N}. \quad (\text{A.21})$$

1118 The following lemma justifies the use of the notation  $W^*$  in the wealth dynamics (A.21).

1119 **Lemma A.6.** (Convergence to optimal wealth) Suppose that Assumption A.2 and Assumption A.3 hold. Let  
 1120  $\mathbf{f}_n^*(\cdot, \boldsymbol{\theta}_n^*) \in \mathcal{N}_n$  be the sequence identified in Lemma A.5 such that (A.10) holds. Then the wealth dynamics  
 1121  $W^*(t; \boldsymbol{\theta}_n^*, \mathbf{Y})$  associated with each  $\mathbf{f}_n^*$ , obtained as per (A.21), converges to the true optimal wealth dynamics  
 1122  $W^*(t; \mathbf{p}^*, \mathbf{Y})$  as  $n \rightarrow \infty$  almost surely. In more detail, we have

$$1123 \quad \lim_{n \rightarrow \infty} W^*(t_m^-; \boldsymbol{\theta}_n^*, \mathbf{Y}) = W^*(t_m^-; \mathbf{p}^*, \mathbf{Y}) \quad \text{a.s.}, \quad \forall t_m \in \mathcal{T}, \quad (\text{A.22})$$

1124 and

$$1125 \quad \lim_{n \rightarrow \infty} W^*(T; \boldsymbol{\theta}_n^*, \mathbf{Y}) = W^*(T; \mathbf{p}^*, \mathbf{Y}) \quad \text{a.s.} \quad (\text{A.23})$$

1126 *Proof.* Note that (A.23) is stated separately since the terminal time  $T$  is not a rebalancing time (see (3.1)) and  
 1127 the terminal wealth is critical in the evaluation of the objective functional.

1128 At the start of the time horizon  $[t_0, T]$ , we are given the initial wealth  $W(t_0^-) = w_0 > 0$ . Therefore, at the  
 1129 first rebalancing time  $t_0 \in \mathcal{T}$ , the wealth available for investment does not depend on the control, so that

$$1130 \quad w_0^+ := w_0 + q(t_0) = W^*(t_0^+; \boldsymbol{\theta}_n^*, \mathbf{Y}) = W^*(t_0^+; \mathbf{p}^*, \mathbf{Y}), \quad \forall n \in \mathbb{N}. \quad (\text{A.24})$$

1131 Using dynamics (A.20) and (A.21) to compare the wealth at time  $t_0 + \Delta t = t_1 \in \mathcal{T}$ , we have

$$1132 \quad \lim_{n \rightarrow \infty} W^*(t_1^-; \boldsymbol{\theta}_n^*, \mathbf{Y}) - W^*(t_1^-; \mathbf{p}^*, \mathbf{Y}) = w_0^+ \cdot \sum_{i=1}^{N_a} \left[ \lim_{n \rightarrow \infty} f_{n,i}^*(t_0, w_0^+; \boldsymbol{\theta}_n^*) - p_i^*(t_0, w_0^+) \right] \cdot Y_i(t_0) \\ 1133 \quad = 0 \quad \text{a.s.}, \quad (\text{A.25})$$

1134 which follows from Lemma A.5 and the fact that  $Y_i(t_0) < \infty$  a.s. by assumption (see definition (3.6)).

1135 For purposes of induction, assume that at some  $t_m \in \mathcal{T}$ , we have

$$1136 \quad \lim_{n \rightarrow \infty} W^*(t_m^-; \boldsymbol{\theta}_n^*, \mathbf{Y}) = W^*(t_m^-; \mathbf{p}^*, \mathbf{Y}) \quad \text{a.s.} \quad (\text{A.26})$$

1137 If (A.26) holds, then we have

$$1138 \quad \lim_{n \rightarrow \infty} W^*(t_m^+; \boldsymbol{\theta}_n^*, \mathbf{Y}) = \lim_{n \rightarrow \infty} [W^*(t_m^-; \boldsymbol{\theta}_n^*, \mathbf{Y}) + q(t_m)] = W^*(t_m^+; \mathbf{p}^*, \mathbf{Y}) \quad \text{a.s.}, \quad (\text{A.27})$$

1139 as well as

$$1140 \quad \lim_{n \rightarrow \infty} |f_{n,i}^*(t_m, W^*(t_m^+; \boldsymbol{\theta}_n^*, \mathbf{Y}); \boldsymbol{\theta}_n^*) - p_i^*(t_m, W^*(t_m^+; \mathbf{p}^*, \mathbf{Y}))| \\ 1141 \quad \leq \lim_{n \rightarrow \infty} |f_{n,i}^*(t_m, W^*(t_m^+; \boldsymbol{\theta}_n^*, \mathbf{Y}); \boldsymbol{\theta}_n^*) - p_i^*(t_m, W^*(t_m^+; \boldsymbol{\theta}_n^*, \mathbf{Y}))| \\ 1142 \quad + \lim_{n \rightarrow \infty} |p_i^*(t_m, W^*(t_m^+; \boldsymbol{\theta}_n^*, \mathbf{Y})) - p_i^*(t_m, W^*(t_m^+; \mathbf{p}^*, \mathbf{Y}))| \\ 1143 \quad \leq \lim_{n \rightarrow \infty} \sup_{\phi \in \mathcal{D}_\phi} |f_{n,i}^*(\phi; \boldsymbol{\theta}_n^*) - p_i^*(\phi)| \\ 1144 \quad = 0 \quad \text{a.s.}, \quad \forall i = 1, \dots, N_a, \quad (\text{A.28})$$

1145 which is a consequence of Lemma A.5 and the continuity of  $\mathbf{p}^* \in C(\mathcal{D}_\phi, \mathcal{Z})$ . From (A.27) and (A.28), we  
 1146 therefore conclude that

$$\lim_{n \rightarrow \infty} |W^*(t_m^+; \boldsymbol{\theta}_n^*, \mathbf{Y}) \cdot f_{n,i}^*(t_m, W^*(t_m^+; \boldsymbol{\theta}_n^*, \mathbf{Y}); \boldsymbol{\theta}_n^*) - W^*(t_m^+; \mathbf{p}^*, \mathbf{Y}) \cdot p_i^*(t_m, W^*(t_m^+; \mathbf{p}^*, \mathbf{Y}))| \\ = 0 \quad \text{a.s.}, \quad \forall i = 1, \dots, N_a. \quad (\text{A.29})$$

1147 Using dynamics (A.20) and (A.21) to compare the wealth at time  $t_m + \Delta t = t_{m+1}$ , we have

$$\begin{aligned}
1148 \quad \lim_{n \rightarrow \infty} W^*(t_{m+1}^-; \boldsymbol{\theta}_n^*, \mathbf{Y}) - W^*(t_{m+1}^-; \mathbf{p}^*, \mathbf{Y}) &= \lim_{n \rightarrow \infty} W^*(t_m^+; \boldsymbol{\theta}_n^*, \mathbf{Y}) \cdot \sum_{i=1}^{N_a} f_{n,i}^*(t_m, W^*(t_m^+; \boldsymbol{\theta}_n^*, \mathbf{Y}); \boldsymbol{\theta}_n^*) \cdot Y_i(t_m) \\
1149 &\quad - W^*(t_m^+; \mathbf{p}^*, \mathbf{Y}) \cdot \sum_{i=1}^{N_a} p_i^*(t_m, W^*(t_m^+; \mathbf{p}^*, \mathbf{Y})) \cdot Y_i(t_m) \\
1150 &= 0 \quad \text{a.s.}, \tag{A.30}
\end{aligned}$$

1151 which follows from (A.29) and  $Y_i(t_m) < \infty$  a.s. By induction, we therefore conclude that (A.22) holds if  
1152  $t_{m+1} \in \mathcal{T}$  (i.e. if  $m < N_{rb} - 1$ ), and (A.23) holds in the case where  $t_{m+1} = t_{N_{rb}} = T$  (i.e.  $m = N_{rb} - 1$ ).  $\square$

1153 The following lemma establishes the convergence of the sequence of objective functionals using the NN  
1154 approximations identified in Lemma A.5.

1155 **Lemma A.7.** (*Convergence of objective functionals*) Suppose that Assumption A.2 and Assumption A.3 hold.  
1156 Let  $\mathbf{f}_n^*(\cdot, \boldsymbol{\theta}_n^*) \in \mathcal{N}_n$  be the sequence identified in Lemma A.5 such that (A.10) holds. Then

$$1157 \quad \lim_{n \rightarrow \infty} J_n(\boldsymbol{\theta}_n^*, \xi; t_0, w_0) = J(\mathbf{p}^*, \xi; t_0, w_0), \quad \forall \xi \in \mathbb{R}, \tag{A.31}$$

1158 where  $J_n$  is defined in (4.9), and  $J$  is defined in (4.4).

1159 *Proof.* Let  $\xi \in \mathbb{R}$  be arbitrary. By Lemma A.6 and the continuity of  $F$ , we have

$$1160 \quad \lim_{n \rightarrow \infty} F(W^*(T; \boldsymbol{\theta}_n^*, \mathbf{Y}), \xi) = F(W^*(T; \mathbf{p}^*, \mathbf{Y}), \xi) \quad \text{a.s.} \tag{A.32}$$

1161 Therefore, by using the boundedness of wealth as per Assumption A.3, the dominated convergence theorem  
1162 gives

$$1163 \quad \lim_{n \rightarrow \infty} E^{t_0, w_0} [F(W^*(T; \boldsymbol{\theta}_n^*, \mathbf{Y}), \xi)] = E^{t_0, w_0} [F(W^*(T; \mathbf{p}^*, \mathbf{Y}), \xi)]. \tag{A.33}$$

1164 Similarly, by the continuity of  $G$ , Lemma A.6, the boundedness of wealth and the dominated convergence  
1165 theorem, we have

$$\begin{aligned}
1166 &\quad \lim_{n \rightarrow \infty} E^{t_0, w_0} [G(W^*(T; \boldsymbol{\theta}_n^*, \mathbf{Y}), E^{t_0, w_0} [W^*(T; \boldsymbol{\theta}_n^*, \mathbf{Y})], w_0, \xi)] \\
1167 &= E^{t_0, w_0} [G(W^*(T; \mathbf{p}^*, \mathbf{Y}), E^{t_0, w_0} [W^*(T; \mathbf{p}^*, \mathbf{Y})], w_0, \xi)]. \tag{A.34}
\end{aligned}$$

1168 Finally, using the definitions of  $J$  in (4.4) and  $J_n$  in (4.9), we combine (A.33) and (A.34) to conclude (A.31).  $\square$

## 1169 Proof of Theorem 5.1

1170 Using the preceding results, we are finally in the position to prove Theorem 5.1. Note that this proof also  
1171 motivates the use of the notation  $\mathbf{f}_n^*(\cdot, \boldsymbol{\theta}_n^*)$  and its associated wealth  $W^*(T; \boldsymbol{\theta}_n^*, \mathbf{Y})$  for the sequence of NNs  
1172 identified in Lemma A.5 and subsequently used in Lemmas A.6 and A.7 above.

1173 Since  $\xi \rightarrow F(w, \xi)$  and  $\xi \rightarrow G(w, x, w_0, \xi)$  are convex by Assumption A.2, and the convexity is preserved  
1174 by taking the expectation of  $F$ , we have the result that  $\xi \rightarrow J_n(\boldsymbol{\theta}_n, \xi; t_0, w_0)$  and  $\xi \rightarrow J(\mathbf{p}, \xi; t_0, w_0)$  are also  
1175 convex, so that the infimum over  $\xi \in \mathbb{R}$  in each case can be attained and is unique. With  $\mathbf{p}^*$  still denoting the  
1176 optimal control, define  $\xi^*$  as the value

$$1177 \quad \xi^* := \inf_{\xi \in \mathbb{R}} J(\mathbf{p}^*, \xi; t_0, w_0). \tag{A.35}$$

1178 Since  $\mathcal{N}_n \subset C(\mathcal{D}_\phi, \mathcal{Z})$ , we have, for all  $\xi \in \mathbb{R}$  and all  $n \in \mathbb{N}$ ,

$$1179 \quad \inf_{\boldsymbol{\theta}_n \in \mathbb{R}^{\nu_n}} J_n(\boldsymbol{\theta}_n, \xi; t_0, w_0) = \inf_{\mathbf{f}_n(\cdot; \boldsymbol{\theta}_n) \in \mathcal{N}_n} J(\mathbf{f}_n, \xi; t_0, w_0) \geq \inf_{\mathbf{p} \in C(\mathcal{D}_\phi, \mathcal{Z})} J(\mathbf{p}, \xi; t_0, w_0). \tag{A.36}$$

1180 Taking the infimum in (A.36) over  $\xi \in \mathbb{R}$ , and exchanging the order of minimization, we therefore have

$$\begin{aligned}
1181 \quad \inf_{(\boldsymbol{\theta}_n, \xi) \in \mathbb{R}^{\nu_n+1}} J_n(\boldsymbol{\theta}_n, \xi; t_0, w_0) &= \inf_{\boldsymbol{\theta}_n \in \mathbb{R}^{\nu_n}} \inf_{\xi \in \mathbb{R}} J_n(\boldsymbol{\theta}_n, \xi; t_0, w_0) \\
1182 \quad &\geq \inf_{\boldsymbol{p} \in C(\mathcal{D}_\phi, \mathcal{Z})} \inf_{\xi \in \mathbb{R}} J(\boldsymbol{p}, \xi; t_0, w_0), \quad \forall n \in \mathbb{N}. \quad (\text{A.37})
\end{aligned}$$

1183 Taking limits in (A.37), we obtain

$$1184 \quad \lim_{n \rightarrow \infty} \inf_{(\boldsymbol{\theta}_n, \xi) \in \mathbb{R}^{\nu_n+1}} J_n(\boldsymbol{\theta}_n, \xi; t_0, w_0) \geq \inf_{\xi \in \mathbb{R}} \inf_{\boldsymbol{p} \in C(\mathcal{D}_\phi, \mathcal{Z})} J(\boldsymbol{p}, \xi; t_0, w_0). \quad (\text{A.38})$$

1185 Now consider specifically the sequence  $\boldsymbol{f}_n^*(\cdot, \boldsymbol{\theta}_n^*)$  identified in Lemma A.5 and the value  $\xi^*$  in (A.35). Since  
1186  $\boldsymbol{f}_n^*(\cdot, \boldsymbol{\theta}_n^*) \in \mathcal{N}_n$  (so that  $\boldsymbol{\theta}_n^* \in \mathbb{R}^{\nu_n}$ ) and  $\xi^* \in \mathbb{R}$ , we have

$$1187 \quad \inf_{(\boldsymbol{\theta}_n, \xi) \in \mathbb{R}^{\nu_n+1}} J_n(\boldsymbol{\theta}_n, \xi; t_0, w_0) \leq J_n(\boldsymbol{\theta}_n^*, \xi^*; t_0, w_0), \quad \forall n \in \mathbb{N}. \quad (\text{A.39})$$

1188 By Lemma A.7, we have

$$1189 \quad \lim_{n \rightarrow \infty} J_n(\boldsymbol{\theta}_n^*, \xi^*; t_0, w_0) = J(\boldsymbol{p}^*, \xi^*; t_0, w_0), \quad \text{where } \xi^* \text{ is given by (A.35)}. \quad (\text{A.40})$$

1190 Therefore, taking limits in (A.39) and using (A.40), we obtain the inequality

$$\begin{aligned}
1191 \quad \lim_{n \rightarrow \infty} \inf_{(\boldsymbol{\theta}_n, \xi) \in \mathbb{R}^{\nu_n+1}} J_n(\boldsymbol{\theta}_n, \xi; t_0, w_0) &\leq \lim_{n \rightarrow \infty} J_n(\boldsymbol{\theta}_n^*, \xi^*; t_0, w_0) \\
1192 \quad &= J(\boldsymbol{p}^*, \xi^*; t_0, w_0) \\
1193 \quad &= \inf_{\xi \in \mathbb{R}} \inf_{\boldsymbol{p} \in C(\mathcal{D}_\phi, \mathcal{Z})} J(\boldsymbol{p}, \xi; t_0, w_0). \quad (\text{A.41})
\end{aligned}$$

1194 Combining (A.38) and (A.41), we therefore have equality in both (A.38) and (A.41), and obtain

$$1195 \quad \lim_{n \rightarrow \infty} \inf_{(\boldsymbol{\theta}_n, \xi) \in \mathbb{R}^{\nu_n+1}} J_n(\boldsymbol{\theta}_n, \xi; t_0, w_0) = \inf_{\xi \in \mathbb{R}} \inf_{\boldsymbol{p} \in C(\mathcal{D}_\phi, \mathcal{Z})} J(\boldsymbol{p}, \xi; t_0, w_0), \quad (\text{A.42})$$

1196 which concludes the proof of Theorem 5.1. Finally, the notation  $\boldsymbol{f}_n^*(\cdot, \boldsymbol{\theta}_n^*)$  in Lemma A.5 is motivated by the  
1197 fact that equality holds in (A.41).  $\square$

## 1198 A.4: Proof of Theorem 5.2

1199 We start with the following auxiliary result, which is essentially a version of the law of large numbers applicable  
1200 to the current setting.

1201 **Lemma A.8.** (*Applicable version of the law of large numbers*) Suppose that Assumption A.2, Assumption A.3  
1202 and Assumption A.4 hold. Then

$$1203 \quad \sup_{\boldsymbol{\theta}_n \in \mathbb{R}^{\nu_n}} \left| \frac{1}{n} \sum_{j=1}^n W^{(j)}(T; \boldsymbol{\theta}_n, \mathcal{Y}_n) - E^{t_0, w_0} [W(T; \boldsymbol{\theta}_n, \boldsymbol{Y})] \right| \xrightarrow{P} 0, \text{ as } n \rightarrow \infty, \quad (\text{A.43})$$

1204 and

$$1205 \quad \sup_{(\boldsymbol{\theta}_n, \xi) \in \mathbb{R}^{\nu_n+1}} \left| \frac{1}{n} \sum_{j=1}^n F\left(W^{(j)}(T; \boldsymbol{\theta}_n, \mathcal{Y}_n), \xi\right) - E^{t_0, w_0} [F(W(T; \boldsymbol{\theta}_n, \boldsymbol{Y}), \xi)] \right| \xrightarrow{P} 0, \text{ as } n \rightarrow \infty. \quad (\text{A.44})$$

1206 *Proof.* Since for any fixed number of hidden layers, our NN formulation also requires  $\mathcal{O}(\hbar_n)$  evaluations of the  
1207 exponential function, exactly the same steps as in Tsang and Wong (2020) (specifically, see Corollary 7.4 and  
1208 Theorem 4.3 in Tsang and Wong (2020)) can be used to establish (A.43) and (A.44).  $\square$

1209 The following lemma establishes a required auxiliary result involving the function  $G$ .

1210 **Lemma A.9.** (*Convergence of  $G$  in probability*) Suppose that Assumption A.2, Assumption A.3 and Assumption

1211 A.4 hold. Then

$$\begin{aligned}
1212 \quad & \sup_{(\boldsymbol{\theta}_n, \xi) \in \mathbb{R}^{\nu_n+1}} \left| \frac{1}{n} \sum_{j=1}^n G \left( W^{(j)}(T; \boldsymbol{\theta}_n, \mathcal{Y}_n), \frac{1}{n} \sum_{k=1}^n W^{(k)}(T; \boldsymbol{\theta}_n, \mathcal{Y}_n), w_0, \xi \right) \right. \\
1213 \quad & \left. - E^{t_0, w_0} [G(W(T; \boldsymbol{\theta}_n, \mathbf{Y}), E^{t_0, w_0} [W(T; \boldsymbol{\theta}_n, \mathbf{Y})], w_0, \xi)] \right| \xrightarrow{P} 0, \quad (\text{A.45})
\end{aligned}$$

1214 as  $n \rightarrow \infty$ .

1215 *Proof.* For given values of  $\xi \in \mathbb{R}$ ,  $w_0 > 0$  and  $w \in \mathbb{R}$ , consider the function  $x \rightarrow G(x, w, w_0, \xi)$ . By the results  
1216 of Lemma A.8, we have

$$1217 \quad \sup_{(\boldsymbol{\theta}_n, \xi) \in \mathbb{R}^{\nu_n+1}} \left| \frac{1}{n} \sum_{j=1}^n G \left( W^{(j)}(T; \boldsymbol{\theta}_n, \mathcal{Y}_n), w, w_0, \xi \right) - E^{t_0, w_0} [G(W(T; \boldsymbol{\theta}_n, \mathbf{Y}), w, w_0, \xi)] \right| \xrightarrow{P} 0, \quad (\text{A.46})$$

as  $n \rightarrow \infty$ . Keeping  $x$  fixed, consider the function  $w \rightarrow G(x, w, w_0, \xi) : [0, w_{max}] \rightarrow \mathbb{R}$ . Since  $G$  is continuous, there exists a sequence of functions  $(G_m)_{m \in \mathbb{N}}$ , where for each  $m \in \mathbb{N}$ , the function  $w \rightarrow G_m(x, w, w_0, \xi) : [0, w_{max}] \rightarrow \mathbb{R}$  is  $L_m$ -Lipschitz, such that  $(G_m)$  converges uniformly to  $G$  on  $[0, w_{max}]$  - see for example Miculescu (2000). Therefore, for an arbitrary value of  $\epsilon > 0$ , there exists a sufficiently large value  $\tilde{m} \in \mathbb{N}$  such that

$$|G_{\tilde{m}}(x, w, w_0, \xi) - G(x, w, w_0, \xi)| < \frac{\epsilon}{2}, \quad \forall w \in [0, w_{max}]. \quad (\text{A.47})$$

1218 Observing that  $\frac{1}{n} \sum_{j=1}^n W^{(j)}(T; \boldsymbol{\theta}_n, \mathcal{Y}_n) \in [0, w_{max}]$  and by the monotonicity of expectation we also have  
1219  $E^{t_0, w_0} [W(T; \boldsymbol{\theta}_n, \mathbf{Y})] \in [0, w_{max}]$ , we use (A.47) to obtain

$$\begin{aligned}
1220 \quad & \left| G_{\tilde{m}} \left( x, \frac{1}{n} \sum_{j=1}^n W^{(j)}(T; \boldsymbol{\theta}_n, \mathcal{Y}_n), w_0, \xi \right) - G \left( x, \frac{1}{n} \sum_{j=1}^n W^{(j)}(T; \boldsymbol{\theta}_n, \mathcal{Y}_n), w_0, \xi \right) \right| \\
1221 \quad & + \left| G_{\tilde{m}}(x, E^{t_0, w_0} [W(T; \boldsymbol{\theta}_n, \mathbf{Y})], w_0, \xi) - G(x, E^{t_0, w_0} [W(T; \boldsymbol{\theta}_n, \mathbf{Y})], w_0, \xi) \right| \\
1222 \quad & < \epsilon, \quad (\text{A.48})
\end{aligned}$$

1223 for any given values of  $\xi \in \mathbb{R}$  and  $w_0 > 0$ . In addition, since  $G_{\tilde{m}}$  is  $L_{\tilde{m}}$ -Lipschitz, we have

$$\begin{aligned}
1224 \quad & \left| G_{\tilde{m}} \left( x, \frac{1}{n} \sum_{j=1}^n W^{(j)}(T; \boldsymbol{\theta}_n, \mathcal{Y}_n), w_0, \xi \right) - G_{\tilde{m}}(x, E^{t_0, w_0} [W(T; \boldsymbol{\theta}_n, \mathbf{Y})], w_0, \xi) \right| \\
1225 \quad & \leq L_{\tilde{m}} \cdot \left| \frac{1}{n} \sum_{j=1}^n W^{(j)}(T; \boldsymbol{\theta}_n, \mathcal{Y}_n) - E^{t_0, w_0} [W(T; \boldsymbol{\theta}_n, \mathbf{Y})] \right|. \quad (\text{A.49})
\end{aligned}$$

1226 Using (A.48) and (A.49) as well as the triangle inequality, we therefore have

$$\begin{aligned}
1227 \quad & \left| G \left( x, \frac{1}{n} \sum_{j=1}^n W^{(j)}(T; \boldsymbol{\theta}_n, \mathcal{Y}_n), w_0, \xi \right) - G(x, E^{t_0, w_0} [W(T; \boldsymbol{\theta}_n, \mathbf{Y})], w_0, \xi) \right| \\
1228 \quad & < \epsilon + L_{\tilde{m}} \cdot \left| \frac{1}{n} \sum_{j=1}^n W^{(j)}(T; \boldsymbol{\theta}_n, \mathcal{Y}_n) - E^{t_0, w_0} [W(T; \boldsymbol{\theta}_n, \mathbf{Y})] \right|, \quad (\text{A.50})
\end{aligned}$$

1229 for any given values of  $\xi \in \mathbb{R}$  and  $w_0 > 0$ . Taking the supremum over  $(\boldsymbol{\theta}_n, \xi) \in \mathbb{R}^{\nu_n+1}$  in (A.50), using the result  
1230 (A.43) from Lemma A.8 as well as the fact that  $\epsilon > 0$  was arbitrary, we therefore have

$$1231 \quad \sup_{(\boldsymbol{\theta}_n, \xi) \in \mathbb{R}^{\nu_n+1}} \left| G \left( x, \frac{1}{n} \sum_{k=1}^n W^{(k)}(T; \boldsymbol{\theta}_n, \mathcal{Y}_n), w_0, \xi \right) - G(x, E^{t_0, w_0} [W(T; \boldsymbol{\theta}_n, \mathbf{Y})], w_0, \xi) \right| \xrightarrow{P} 0. \quad (\text{A.51})$$



1232 The results (A.46) and (A.51), together with the triangle inequality, therefore gives

$$\begin{aligned}
1233 & \sup_{(\boldsymbol{\theta}_n, \xi) \in \mathbb{R}^{\nu_n+1}} \left| \frac{1}{n} \sum_{j=1}^n G \left( W^{(j)}(T; \boldsymbol{\theta}_n, \mathcal{Y}_n), \frac{1}{n} \sum_{k=1}^n W^{(k)}(T; \boldsymbol{\theta}_n, \mathcal{Y}_n), w_0, \xi \right) \right. \\
1234 & \quad \left. - E^{t_0, w_0} [G(W(T; \boldsymbol{\theta}_n, \mathbf{Y}), E^{t_0, w_0} [W(T; \boldsymbol{\theta}_n, \mathbf{Y})], w_0, \xi)] \right| \\
1235 & \leq \frac{1}{n} \sum_{j=1}^n \sup_{(\boldsymbol{\theta}_n, \xi) \in \mathbb{R}^{\nu_n+1}} \left| \frac{1}{n} \sum_{j=1}^n G \left( W^{(j)}(T; \boldsymbol{\theta}_n, \mathcal{Y}_n), \frac{1}{n} \sum_{k=1}^n W^{(k)}(T; \boldsymbol{\theta}_n, \mathcal{Y}_n), w_0, \xi \right) \right. \\
1236 & \quad \left. - G \left( W^{(j)}(T; \boldsymbol{\theta}_n, \mathcal{Y}_n), E^{t_0, w_0} [W(T; \boldsymbol{\theta}_n, \mathbf{Y})], w_0, \xi \right) \right| \\
1237 & + \sup_{(\boldsymbol{\theta}_n, \xi) \in \mathbb{R}^{\nu_n+1}} \left| \frac{1}{n} \sum_{j=1}^n G \left( W^{(j)}(T; \boldsymbol{\theta}_n, \mathcal{Y}_n), E^{t_0, w_0} [W(T; \boldsymbol{\theta}_n, \mathbf{Y})], w_0, \xi \right) \right. \\
1238 & \quad \left. - E^{t_0, w_0} [G(W(T; \boldsymbol{\theta}_n, \mathbf{Y}), E^{t_0, w_0} [W(T; \boldsymbol{\theta}_n, \mathbf{Y})], w_0, \xi)] \right| \\
1239 & \xrightarrow{P} 0 \quad \text{as } n \rightarrow \infty. \tag{A.52}
\end{aligned}$$

1240 □

## 1241 Proof of Theorem 5.2

1242 The expression in (5.2), together with the triangle inequality, imply that

$$\begin{aligned}
1243 & \left| \inf_{(\boldsymbol{\theta}_n, \xi) \in \mathbb{R}^{\nu_n+1}} \hat{J}_n(\boldsymbol{\theta}_n, \xi; t_0, w_0, \mathcal{Y}_n) - \inf_{\xi \in \mathbb{R}} \inf_{\mathbf{p} \in C(\mathcal{D}_\phi, \mathcal{Z})} J(\mathbf{p}, \xi; t_0, w_0) \right| \\
1244 & \leq \left| \inf_{(\boldsymbol{\theta}_n, \xi) \in \mathbb{R}^{\nu_n+1}} \hat{J}_n(\boldsymbol{\theta}_n, \xi; t_0, w_0, \mathcal{Y}_n) - \inf_{(\boldsymbol{\theta}_n, \xi) \in \mathbb{R}^{\eta_n+1}} J_n(\boldsymbol{\theta}_n, \xi; t_0, w_0) \right| \tag{A.53}
\end{aligned}$$

$$\begin{aligned}
1245 & + \left| \inf_{(\boldsymbol{\theta}_n, \xi) \in \mathbb{R}^{\nu_n+1}} J_n(\boldsymbol{\theta}_n, \xi; t_0, w_0) - \inf_{\xi \in \mathbb{R}} \inf_{\mathbf{p} \in C(\mathcal{D}_\phi, \mathcal{Z})} J(\mathbf{p}, \xi; t_0, w_0) \right|. \tag{A.54}
\end{aligned}$$

1246 Using the definitions of  $\hat{J}_n(\boldsymbol{\theta}_n, \xi; t_0, w_0, \mathcal{Y}_n)$  in (4.15) and  $J_n(\boldsymbol{\theta}_n, \xi; t_0, w_0)$  in (4.9), the expression (A.53)  
1247 gives

$$\begin{aligned}
1248 & \left| \inf_{(\boldsymbol{\theta}_n, \xi) \in \mathbb{R}^{\nu_n+1}} \hat{J}_n(\boldsymbol{\theta}_n, \xi; t_0, w_0, \mathcal{Y}_n) - \inf_{(\boldsymbol{\theta}_n, \xi) \in \mathbb{R}^{\eta_n+1}} J_n(\boldsymbol{\theta}_n, \xi; t_0, w_0) \right| \\
1249 & \leq \sup_{(\boldsymbol{\theta}_n, \xi) \in \mathbb{R}^{\nu_n+1}} \left| \hat{J}_n(\boldsymbol{\theta}_n, \xi; t_0, w_0, \mathcal{Y}_n) - J_n(\boldsymbol{\theta}_n, \xi; t_0, w_0) \right| \\
1250 & \leq \sup_{(\boldsymbol{\theta}_n, \xi) \in \mathbb{R}^{\nu_n+1}} \left| \frac{1}{n} \sum_{j=1}^n F \left( W^{(j)}(T; \boldsymbol{\theta}_n, \mathcal{Y}_n), \xi \right) - E^{t_0, w_0} [F(W(T; \boldsymbol{\theta}_n, \mathbf{Y}), \xi)] \right| \tag{A.55}
\end{aligned}$$

$$\begin{aligned}
1251 & + \sup_{(\boldsymbol{\theta}_n, \xi) \in \mathbb{R}^{\nu_n+1}} \left| \frac{1}{n} \sum_{j=1}^n G \left( W^{(j)}(T; \boldsymbol{\theta}_n, \mathcal{Y}_n), \frac{1}{n} \sum_{k=1}^n W^{(k)}(T; \boldsymbol{\theta}_n, \mathcal{Y}_n), w_0, \xi \right) \right. \\
1252 & \quad \left. - E^{t_0, w_0} [G(W(T; \boldsymbol{\theta}_n, \mathbf{Y}), E^{t_0, w_0} [W(T; \boldsymbol{\theta}_n, \mathbf{Y})], w_0, \xi)] \right|. \tag{A.56}
\end{aligned}$$

1253 As per Lemma A.8 and Lemma A.9, (A.55) and (A.56) converge to zero in probability as  $n \rightarrow \infty$ . As a result,  
1254 since (A.53) therefore converges to zero in probability as  $n \rightarrow \infty$  and, by Theorem 5.1, (A.54) converges to zero  
1255 as  $n \rightarrow \infty$ , we conclude that the result (5.2) of Theorem 5.2 holds. □

## 1256 Appendix B: NN approach: Selected practical considerations

1257 We summarize some practical considerations with respect to the NN approach:

1258 (i) Constructing training and testing datasets  $\mathcal{Y}_n$  and  $\mathcal{Y}_n^{test}$ : Since these sets correspond to finite samples of  
1259  $\mathbf{Y}$  and  $\mathbf{Y}^{test}$ , any data generation technique generating paths of underlying asset returns can be used for  
1260 the construction of training and testing data sets. As illustrated in Section 6, data generation techniques  
1261 like (i) Monte Carlo simulation of parametric asset dynamics, (ii) block bootstrap resampling of empirical  
1262 returns, or for example (iii) GAN-generated synthetic returns can all be employed without difficulty, but  
1263 we emphasize that the approach remains agnostic regarding the underlying data generation methodology.  
1264 Note that the underlying data generation assumptions typically differ for  $\mathcal{Y}_n$  and  $\mathcal{Y}_n^{test}$ , respectively,  
1265 depending on for example the time periods of empirical data considered for in-sample and out-of-sample  
1266 testing.

1267 As for the number of paths  $n$  in each of  $\mathcal{Y}_n$  and  $\mathcal{Y}_n^{test}$ , experiments show that in the case of measures of  
1268 tail risk in the objectives such as CVaR (see (3.15)), a significantly larger number of paths are required  
1269 in order to obtain a sufficiently large sample of tail outcomes in the training and testing data, than for  
1270 example in cases where variance is the risk measure. To give a concrete examples, at least 2 million paths  
1271 in the training set of the NN in Subsection 6.2 is required to produce reliable results for the CVaR, whereas  
1272 1 million paths in the training set of the NN in Subsection 6.1 are more than sufficient to obtain reliable  
1273 results.

1274 (ii) Depth (number of hidden layers  $\mathcal{L}^h$ ) and width (number of nodes in each hidden layer  $h(n)$ ) of the NN: As  
1275 the examples in Section 6 show, remarkably accurate can be obtained with NNs no deeper than 2 hidden  
1276 layers and a relatively small number of nodes in each hidden layer. For objectives involving more complex  
1277 investment strategies such as MCV and Mean - Semi-variance (where, even in the case of two assets, the  
1278 behavior of the optimal strategy is clearly more complex than in the case of for example the MV-optimal  
1279 strategy), experiments show that two hidden layers lead to stable and reliable results, with the number  
1280 of hidden nodes in each hidden layer chosen to be slightly more than the number of assets, for example  
1281  $h(n) = N_a + 2$ . For objectives such as DSQ and MV, a single hidden layer is often sufficient.

1282 (iii) Activation functions: As highlighted in Assumption A.1, we use logistic sigmoid activations as a concrete  
1283 example for convergence analysis purposes, but that these theoretical results can be modified for any of  
1284 the commonly-used activations (see for example Sonoda and Murata (2017)). Note that since NNs of one  
1285 or two hidden layers were found to be very effective in solving the problems under consideration, we did  
1286 not encounter any problems related to vanishing or exploding gradients in the case of logistic sigmoid  
1287 activations. However, if deeper NNs are required, activation functions could be changed to e.g. ReLU or  
1288 ELU without affecting the theoretical foundations for the proposed approach.

1289 (iv) For the solution of (4.16) by gradient descent, we used the Gadam algorithm of Granzio et al. (2021).  
1290 This is simply a combination of the Adam algorithm (Kingma and Ba (2015)) with tail iterate averaging  
1291 for improved convergence properties and variance reduction (Mucke et al. (2019); Neu and Rosasco (2018);  
1292 Polyak and Juditsky (1992)). For the Adam algorithm component, the default algorithm parameters of  
1293 Kingma and Ba (2015) performed well in our setting, typically with no more than 50,000 SGD steps. Note  
1294 that the mini-batch size selected depends on the problem to be solved: we found that mini-batch sizes  
1295 of at least 1,000 paths of the training data set  $\mathcal{Y}_n$  are required for measures of tail risk in the objective  
1296 (such as CVaR), since smaller batch sizes typically means that the tail of the returns distribution is not  
1297 sufficiently well represented in choosing the descent direction, leading to unreliable results in ground truth  
1298 analyses.

1299 While the technical results of Section 6 formally do not require continuous differentiability (in addition  
1300 to continuity) of the functions  $F$  and  $G$ , improved convergence properties of the SGD algorithm can  
1301 be obtained if the objective is at least continuously differentiable (see for example Shapiro and Wardi  
1302 (1996)). For implementation purposes, we can therefore smooth objectives like (3.15) in a straightforward  
1303 way, by for example replacing  $\max(x, 0)$  in (3.15) with a continuously differentiable approximation used

in Alexander et al. (2006),

$$\max(x, 0) \simeq \begin{cases} x, & \text{if } x > \lambda_{mcv}, \\ \frac{1}{4\lambda_{mcv}}x^2 + \frac{1}{2}x + \frac{1}{4}\lambda_{mcv}, & \text{if } -\lambda_{mcv} \leq x \leq \lambda_{mcv}, \\ 0, & \text{otherwise,} \end{cases} \quad (\text{B.1})$$

where  $\lambda_{mcv}$  is some small smoothing parameter (e.g.  $\lambda_{mcv} = 10^{-3}$ ).

In addition to considering the smoothing of certain objectives, minor modifications to objective functions to avoid (mathematical) ill-posedness may be desirable in certain situations. For example, in the case of the OSQ objective (3.11), the term  $\epsilon W(\cdot)$  is added to ensure the problem remains well-posed even if  $W(t) \gg \gamma$ . In this case, when implementing the numerical solution, small values of  $\epsilon$  (for example  $\epsilon = 10^{-6}$  was chosen in the numerical results of Section 6) do not have a noticeable effect on either the summary statistics or the optimal controls.

## Appendix C: Additional parameters for numerical results

In this appendix, additional parameters related to the numerical results of Section 6 are discussed.

The historical returns data for the basic assets such as the T-bills/bonds and the broad market index were obtained from the CRSP<sup>7</sup>, whereas factor data for Size and Value (see Fama and French (2015, 1992)) were obtained from Kenneth French’s data library<sup>8</sup> (KFDL). The detailed time series sourced for each asset is as follows:

- (i) T30 (30-day Treasury bill): CRSP, monthly returns for 30-day Treasury bill.
- (ii) B10 (10-year Treasury bond): CRSP, monthly returns for 10-year Treasury bond.<sup>9</sup>
- (iii) Market (broad equity market index): CRSP, monthly returns, including dividends and distributions, for a capitalization-weighted index consisting of all domestic stocks trading on major US exchanges (the VWD index).
- (iv) Size (Portfolio of small stocks): KFDL, “Portfolios Formed on Size”, which consists of monthly returns on a capitalization-weighted index consisting of the firms (listed on major US exchanges) with market value of equity, or market capitalization, at or below the 30th percentile (i.e. smallest 30%) of market capitalization values of NYSE-listed firms.
- (v) Value (Portfolio of value stocks): KFDL, “Portfolios Formed on Book-to-Market”, which consists of monthly returns on a capitalization-weighted index of the firms (listed on major US exchanges) consisting of the firms (listed on major US exchanges) with book-to-market value of equity ratios at or above the 70th percentile (i.e. highest 30%) of book-to-market ratios of NYSE-listed firms.

The historical asset returns time series are inflation-adjusted using inflation data from the US Bureau of Labor Statistics<sup>10</sup>.

For the purposes of obtaining the parameters for (6.1) in Subsections (6.1) and (6.2), we use the same calibration methodology as outlined in Dang and Forsyth (2016); Forsyth and Vetzal (2017), and assume the jump dynamics of the Kou (2002) model.

In particular, we assume that in the dynamics (6.1),  $\log \vartheta_i$  has a asymmetric double-exponential distribution,

$$f_{\vartheta_i}(\vartheta_i) = \nu_i \zeta_{i,1} \vartheta_i^{-\zeta_{i,1}-1} \mathbb{I}_{[\vartheta_i \geq 1]}(\vartheta_i) + (1 - \nu_i) \zeta_{i,2} \vartheta_i^{\zeta_{i,2}-1} \mathbb{I}_{[0 \leq \vartheta_i < 1]}(\vartheta_i), \quad (\text{C.1})$$

where  $\nu_i \in [0, 1]$  and  $\zeta_{i,1} > 1, \zeta_{i,2} > 0$ . In (C.1),  $\nu_i$  denotes the probability of an upward jump given that a jump occurs. The resulting parameters are obtained using the filtering technique for the calibration of jump diffusion processes - see Dang and Forsyth (2016); Forsyth and Vetzal (2017) for the relevant methodological

<sup>7</sup>Calculations were based on data from the Historical Indexes 2020©, Center for Research in Security Prices (CRSP), The University of Chicago Booth School of Business. Wharton Research Data Services was used in preparing this article. This service and the data available thereon constitute valuable intellectual property and trade secrets of WRDS and/or its third party suppliers.

<sup>8</sup>See [https://mba.tuck.dartmouth.edu/pages/faculty/ken.french/data\\_library.html](https://mba.tuck.dartmouth.edu/pages/faculty/ken.french/data_library.html)

<sup>9</sup>The 10-year Treasury index was constructed from monthly returns from CRSP back to 1941. The data for 1926-1941 were interpolated from annual returns in Homer and Sylla (2015)

<sup>10</sup>The annual average CPI-U index, which is based on inflation data for urban consumers, were used - see <http://www.bls.gov/cpi>

1342 details. For calibration purposes, a jump threshold equal to 3 has been used in the methodology of Dang and  
 1343 Forsyth (2016).

1344 Table C.1 and Table C.2 summarize the parameters for the asset dynamics for Subsections (6.1) and (6.2),  
 1345 respectively.

**Table C.1:** Calibrated, inflation-adjusted parameters for asset dynamics in Subsection 6.1: Ground truth -  $DSQ(\gamma)$  with continuous rebalancing. In this example, the first asset is assumed to be a risk-free asset, so we set  $\mu_1 = r$ , while the second asset follows jump dynamics. The parametric asset returns are (trivially) uncorrelated, and parameters are based on the inflation-adjusted returns of the T30 and VWD time series, respectively, over the period 1926:01 to 2019:12

Parameter	$\mu_i$	$\sigma_i$	$\lambda_i$	$v_i$	$\zeta_{i,1}$	$\zeta_{i,2}$
Asset 1 (T30)	0.0043	-	-	-	-	-
Asset 2(VWD)	0.0877	0.1459	0.3191	0.2333	4.3608	5.504

1346

**Table C.2:** Calibrated, inflation-adjusted parameters for asset dynamics in Subsection 6.2: Ground truth - problem  $MCV(\rho)$ . In this example, there are two assets with jump dynamics (see Forsyth and Vetzal (2022)), with parameters based on the inflation-adjusted returns of the T30 and VWD time series over the period 1926:01 to 2019:12. The Brownian motions in (6.1) have correlation  $dZ_1 dZ_2 = \rho_{1,2} dt$ .

Parameter	$\mu_i$	$\sigma_i$	$\lambda_i$	$v_i$	$\zeta_{i,1}$	$\zeta_{i,2}$	$\rho_{1,2}$
Asset 1 (T30)	0.0045	0.0130	0.5106	0.3958	65.85	57.75	0.08228
Asset 2(VWD)	0.0877	0.1459	0.3191	0.2333	4.3608	5.504	0.08228

1347